Reviewer 1 Comment 1: Sources of particle number. The authors calculate the particle number contributed by each source based on the corresponding mass (equation 1 in the paper). This is wrong for two reasons. First a significant fraction of the particle mass is secondary (sulfates, nitrates, secondary organic aerosol). When the secondary mass increases, the contribution of the corresponding source to particle number does not. Second, co- agulation involves particles from different sources. It is not clear to which source the authors assign the particle resulting from the coagulation of two particles from different sources. Both of these problems are quite important for ultrafine particle number con-centrations. The errors of this oversimplified approach should be estimated (at least for one period) with careful zero-out analysis (e.g., removing only the ultrafines and not the larger particles to avoid changes in the condensation and coagulation sinks). If the error is significant the corresponding part of the work should be redone or should be replaced with just a description of the contributions to emissions for different size ranges.

Response: We apologize that the methods to calculate particle number were not explained clearly in the first version of the paper. The text on lines 310-325 has been updated to provide more details. The model framework uses a moving sectional approach to conserve particle number and mass while letting particle radius increase due to condensation (Kleeman, Cass, and Eldering 1997). The method to calculate source contributions to number concentration is performed for each moving section individually. Number is explicitly conserved and correctly apportioned to sources in this algorithm.

Each particle source type / moving size bin includes an artificial tracer equal to 1% of the primary particle mass. The mass of this tracer is related to the number of particles by the equation

Tracer_source_i * 100 = N_source_i * 3.14159/6 * Dp_bin * density_source_i

This equation can be easily rearranged to solve for N_source_i as a function of Tracer_source_i in each size bin. Again, since the model uses a moving sectional approach, number and tracer mass are exactly conserved. Condensation/evaporation changes the particle diameter as semi-volatile components move on and off the particle but this does not change Tracer_source_i or N_source_i. The moving sectional approach greatly simplifies the source apportionment of particle number compared to other models that use fixed particle size bins with condensation / evaporation transferring material between bins.

The text on lines 326-337 has been updated to describe how source apportionment calculations handle coagulation. Coagulation is fastest between very small particles and relatively large particles in the atmosphere. The net effect of coagulation is to remove ultrafine particles from the atmosphere as they collide and join the particles larger than 100 nm. This loss mechanism is accurately simulated in the model calculations. The rate of "self-coagulation" between two ultrafine particles that produces a particle still in the ultrafine particle size range is negligible at atmospherically relevant concentrations. Table 2 compares the timescale for 0.01 µm particles coagulating with other 0.01 µm particles and coagulating with 0.1 µm particles based on size distributions measured in a typical suburban environment in a California city (see Figure 1). The coagulation of timescale between two 0.01 µm particles is 209 hrs (8.7 days) while the coagulation timescale between 0.01 µm particles and 0.1 µm particles is 4.4 hours. Therefore, self-coagulation between ultrafine particles smaller than 60 nm is much less significant than coagulation between ultrafine particles and larger particles (acting as a loss mechanism for ultrafine particles in the atmosphere).

Table 2 Time scale for coagulation between 0.01 µm particles with 0.01 µm particles and 0.1 µm particles in a typical suburban environment in California. See Fig 1 for size distribution used for calculations.

Particle size	0.01	0.1
Coagulation Coefficient(cm^3/s)	1.90E-09	2.50E-08
PM Number concentration ($\#/cm^3$)	1.40E+03	5.00E+03
timescale (hours)	208.9	4.4

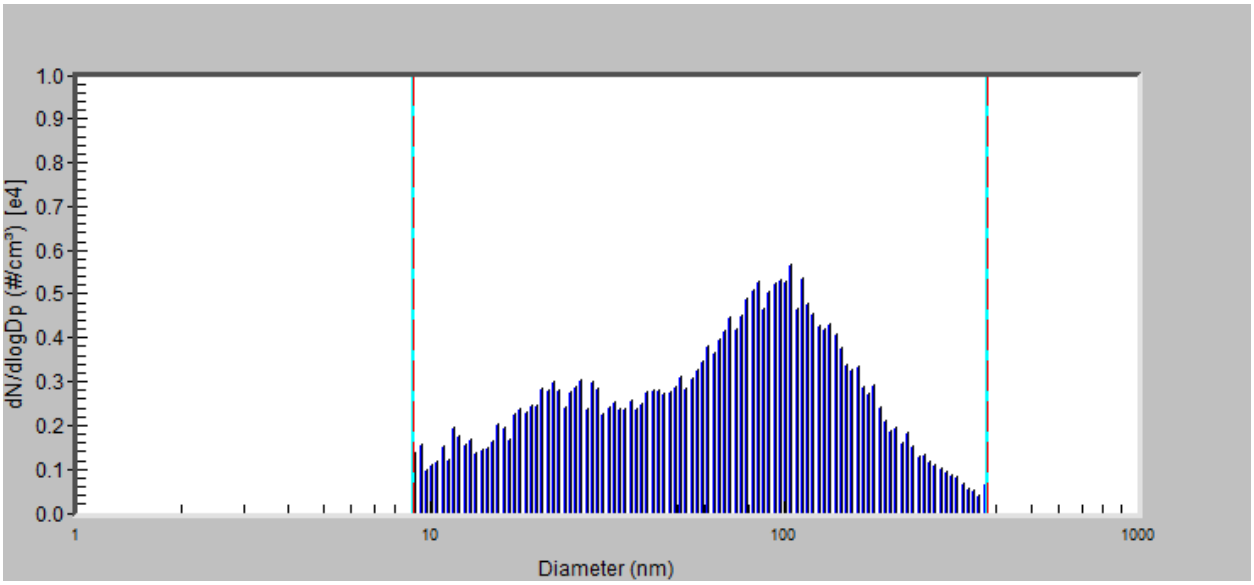

Figure 1 Particle size distribution measured in a typical suburban environment in a California city

Source apportionment calculations treat coagulation events between very small particles and very large particles in a manner analogous to condensation. When two particles coagulate, the mass of the smaller particle is added to the mass of the larger particle. The number concentration of the smaller particle is discarded while the number concentration of the larger particle stays constant. This slightly reduces the accuracy of source apportionment calculations for particle number in the larger size bins because the Tracer_source mass in the larger size bin is no longer proportional to the number concentration from that source. This issue is relatively minor since size bins larger than 1µm that act as the dominant sink during particle coagulation events typically account for less than 5% of the total number concentration.

Perturbation studies were conducted as requested by the reviewer by setting the UFP emissions for on-road gasoline vehicles to zero during the month August 2012. Emissions of gases and emissions of larger particles from on-road vehicles were not changed. The difference between this perturbation simulation vs. the basecase simulation was calculated to estimate the number concentration of particles associated with on-road gasoline vehicles. This "zero-out" concentration is then compared to the standard model source-apportionment calculations in Figure 2 below (shown as Figure 3 in the revised manuscript). The two methods for number source apportionment yield very similar spatial patterns and very similar maximum concentrations of approximately 0.5 kcounts/cm^3. The tracer source apportionment method

accounts for all particle sizes which produces slightly higher concentrations than the zero-out method that only considered particles smaller than 100 nm. This test confirms that the online source apportionment methods for number in the current study work correctly.

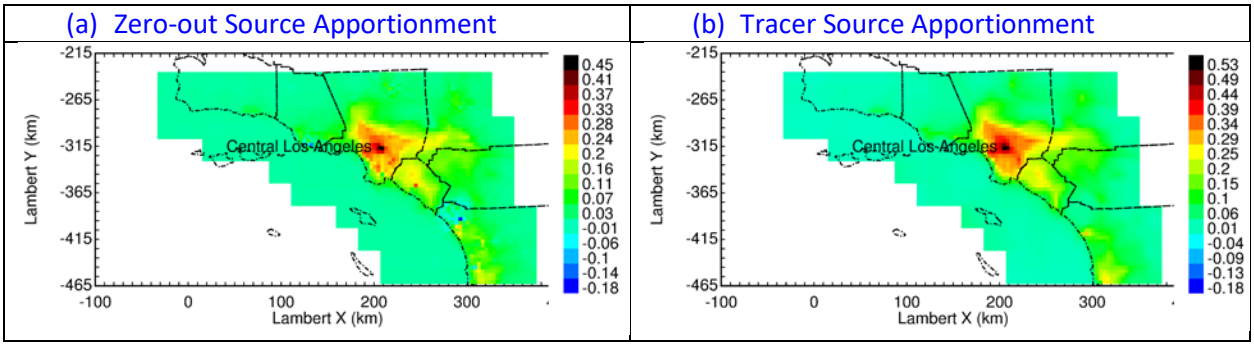

Figure 2 Particle number concentrations associated with on-road gasoline vehicles calculated using the zero-out method and the artificial tracer method in August 2012.

Reviewer 1 Comment 2: Importance of non-residential natural gas combustion as a source of ultrafine particles. This is clearly the most important, but also the most controversial finding of the study. The evidence provided to support this potentially very important result is rather weak and the authors miss a lot of opportunities to strengthen their argument.

The first is the use of size distributions. The predicted size distributions from this source apparently peak in the 10-20 nm size range. There are a lot of available size distribution measurements in the area that can be directly compared with the model predictions. My understanding however is that the measured number size distributions (not immediately next to freeways) peak at the 35-40 nm range (see for example Sowlat et al., 2016). Some of these size distribution measurements are available for the periods that have been simulated so a comparison of size distributions (including sources) could be performed without much effort.

The second is the use of the spatial distribution of particle number. The predicted concentration maps are not shown, but one would expect much higher concentrations near the corresponding major source areas. Traffic should have quite a different spatial pattern. There have been also a lot of particle number distribution measurements in California during the last decade. An effort to test if the predicted patterns match the observed ones would help.

The third is the average diurnal variation. However, this study assumes that the non- residential natural gas emissions have a similar temporal pattern as traffic (Figure S2). So the observed rush-hour peak in particle number that all previous studies assign to traffic, here is explained by natural gas combustion. However, more careful spatio- temporal analysis could help strengthen (or weaken) the conclusion. For example, the predicted morning number peak in Rubidoux in summer does not exist in the measurements. The situation is even worse in midday during the winter suggesting that emissions from this source are clearly overestimated in this area. Is this helpful? Is this area dominated by these emissions or is the sampling site an exception? On the other hand, the model performs well in other areas so one could make the opposite argument site by site. However, without using all the information about predicted patterns in space and time it is difficult to reach a conclusion.

Response: Xue et al. showed that the primary size distribution for natural gas combustion peaks at approximately 20 nm but the size mode grows to approximately 60 nm after 3 hrs of aging in a smog chamber with a representative urban atmosphere consistent of realistic concentrations of VOCs and NOx under realistic UV intensity (Xue et al. 2018). Similar growth occurs in model calculations meaning that the natural gas particles do not stay static at 20 nm in the atmosphere. This point has been clarified on lines 490-491 and in Figure 1 of the revised manuscript. The measurements of larger particles in the atmosphere therefore do not definitively identify sources. Expert opinion is still required to interpret the size distributions and assign them to sources. The results of the current study should help refine those expert opinions in the future.

Many of the spatial patterns measured for airborne particle number concentrations have focused on the gradients around roads (see for example (Zhang et al., 2005;Zhang et al., 2004;Zhu et al., 2002a;Zhu et al., 2002b)). Likewise, the study performed by Solwat et al. (2016) referenced by the reviewer was carried out within 150m of a major freeway and so the reported particle size distributions are dominated by traffic sources. These gradients are impossible to resolve using a regional model with 4km resolution. A limited set of additional simulations were conducted using the WRF/Chem model configured with Large Eddy Simulation (LES) around Oakland California so that spatial scales down to 250m could be examined. Maps of the predicted ultrafine particle mass concentrations for gasoline, diesel, food cooking, wood combustion, and natural gas combustion particles are shown in Figure 3 below (shown as Figure 4 in the revised manuscript). At 250m resolution, ultrafine particles from diesel engines peak on major transportation corridors while ultrafine particles from gasoline vehicles are more diffuse reflecting their increased activity on adjacent surface streets. Ultrafine particles from natural gas combustion are even more diffuse reflecting contributions from area sources across the region. As the spatial resolution decreases to 1km and then 4km, the fine details around roadways are artificially diluted in the larger grid cells. This process shifts the dominant source of ultrafine particles over roadways from diesel engines at 250m resolution to natural gas combustion at 4km resolution. This discussion is now included on lines 363-377 of the revised manuscript.

The ultrafine particle model simulations summarized in Figure 3 are consistent with measurements of particle number in the proximity of roadways which show that the traffic contribution to particle number concentration decays to background levels within 300 m (Zhu, Hinds, Kim, Shen, et al. 2002; Zhu, Hinds, Kim, and Sioutas 2002). The measurements made by Zhu et al. indicate that the traffic contribution to regional number concentration cannot be distinguished from other sources on a regional scale using 4km grid cells which is the focus of this study.

Repeating all of the simulations at 250m resolution is beyond the scope of the current study. We emphasize the regional scope of the simulations in the main text of the revised manuscript to inform the readers about the appropriate interpretation of the current results, and we have also added “regional” to the title of the manuscript.

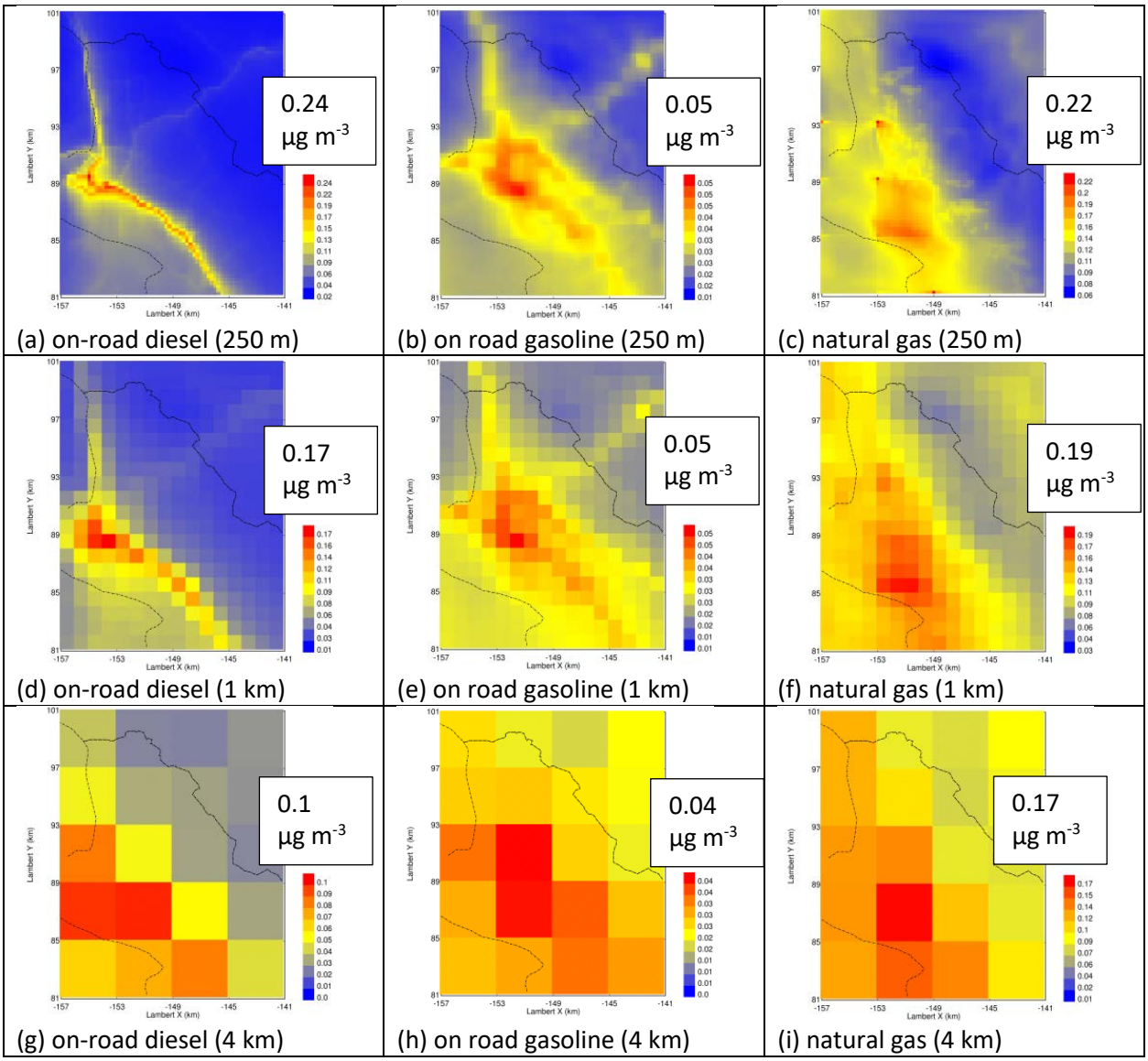

Figure 3: $PM_{0.1}$ mass concentration associated with on-road diesel, on-road gasoline, and natural gas combustion at 250m, 1km, and 4km resolution over Oakland, California.

Hudda et al. (2014) found that particle number concentrations increased by a factor of four to eight downwind of the Los Angeles International Airport (LAX) based on measurements in June-July 2013. Total ground-level number concentrations in the LAX plume reached 60-70 $*10^3$ counts/cm^3. Figure 4 illustrates the predicted number concentration associated with primary emissions (Figures 4a-i) and nucleation (Figure j) averaged over the months Aug-Dec 2012. Figure 4g shows that primary aircraft emissions in the LAX plume are predicted to account for 8 * 10^3 counts/cm^3 and Figure 4j shows that nucleation of aircraft emissions in the LAX plume are predicted to account for 45 * 10^3 counts/cm^3 yielding a total number concentration associated with LAX aircraft of approximately 53 * 10^3 counts/cm^3. Given the 4km spatial resolution of the model calculations, these findings are in good agreement with the measurements by Hudda et al. (2014).

It is noteworthy that military airbases in Figure 4g have significantly higher particle number concentrations due to their use of aviation fuel with higher sulfur content but nucleation plumes are not present downwind of these locations (Figure 4j). Particles emitted from military aircraft are represented as primary emissions in the current model calculations. Future measurements should compare particle number concentrations downwind of civilian and military airports to fully evaluate the impact of aviation fuel sulfur content on ambient ultrafine particle concentrations.

The discussion of the spatial patterns of number concentrations downwind of airports is summarized in Figure 18 and on lines 559-576 of the revised manuscript.

Figure 5 illustrates the predicted particle number concentrations associated with primary sources and nucleation in northern California. The relative importance of sources and the prediction of nucleation downwind of major sulfur emissions are consistent in northern and southern California. Natural gas combustion is a notable strong source of ultrafine particles in both regions due to the widespread use of this fuel in numerous residential, commercial, and industrial applications. In many cases, the natural gas combustion particles contribute strongly to the "urban background' concentrations over most California cities without the formation of individual plumes such as those found downwind of LAX. Future measurements could correlate ambient particle number concentrations and natural gas utilization across multiple cities to evaluate whether natural gas combustion is a significant source of particle number concentration.

The spatial patterns of nucleated particle number concentrations have been summarized on lines 595-620 in the main text of the revised manuscript along with Figures 20 and 21.

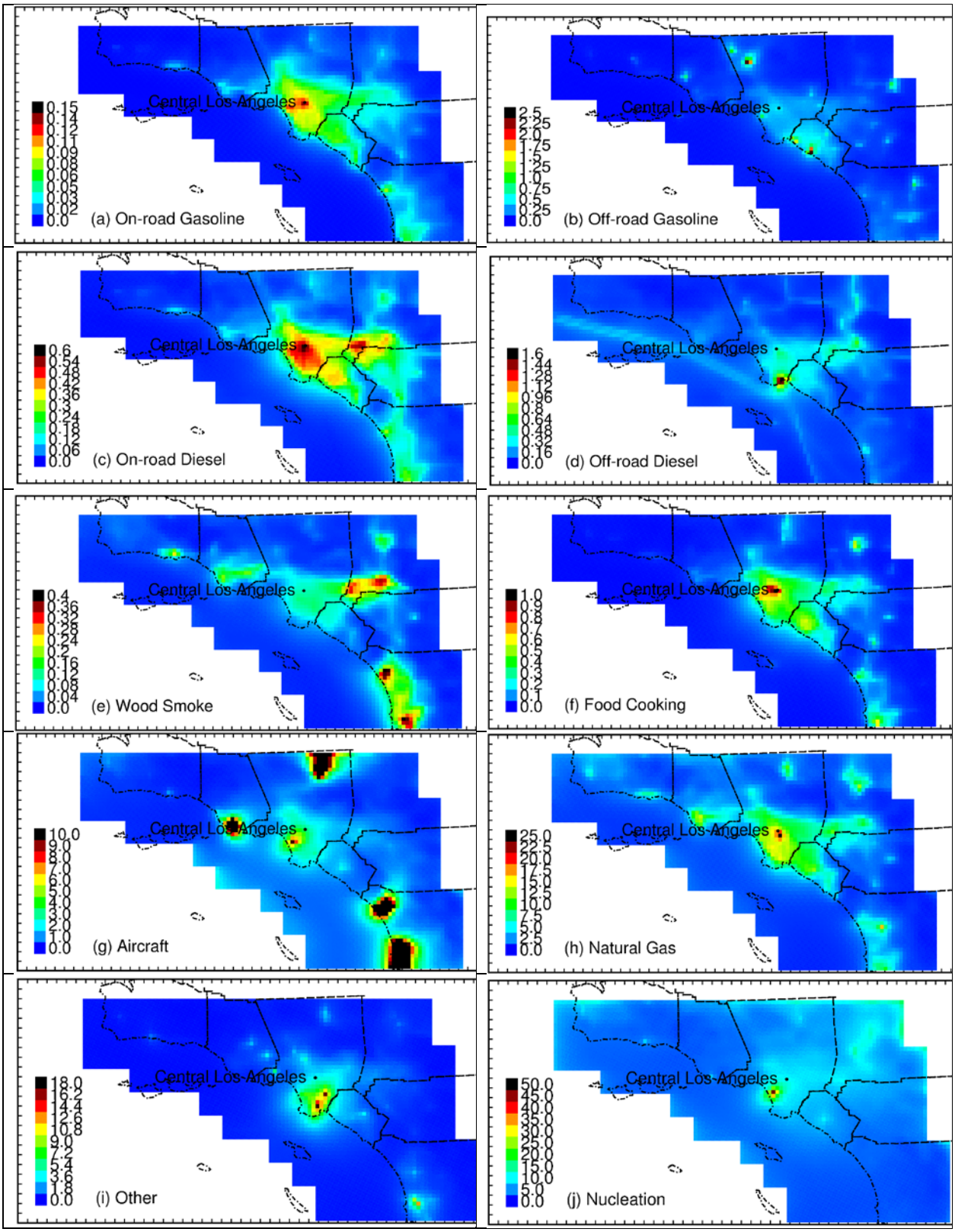

Figure 4. Spatial distribution of particle number from major sources in Southern California (unit: kcount/cm3).

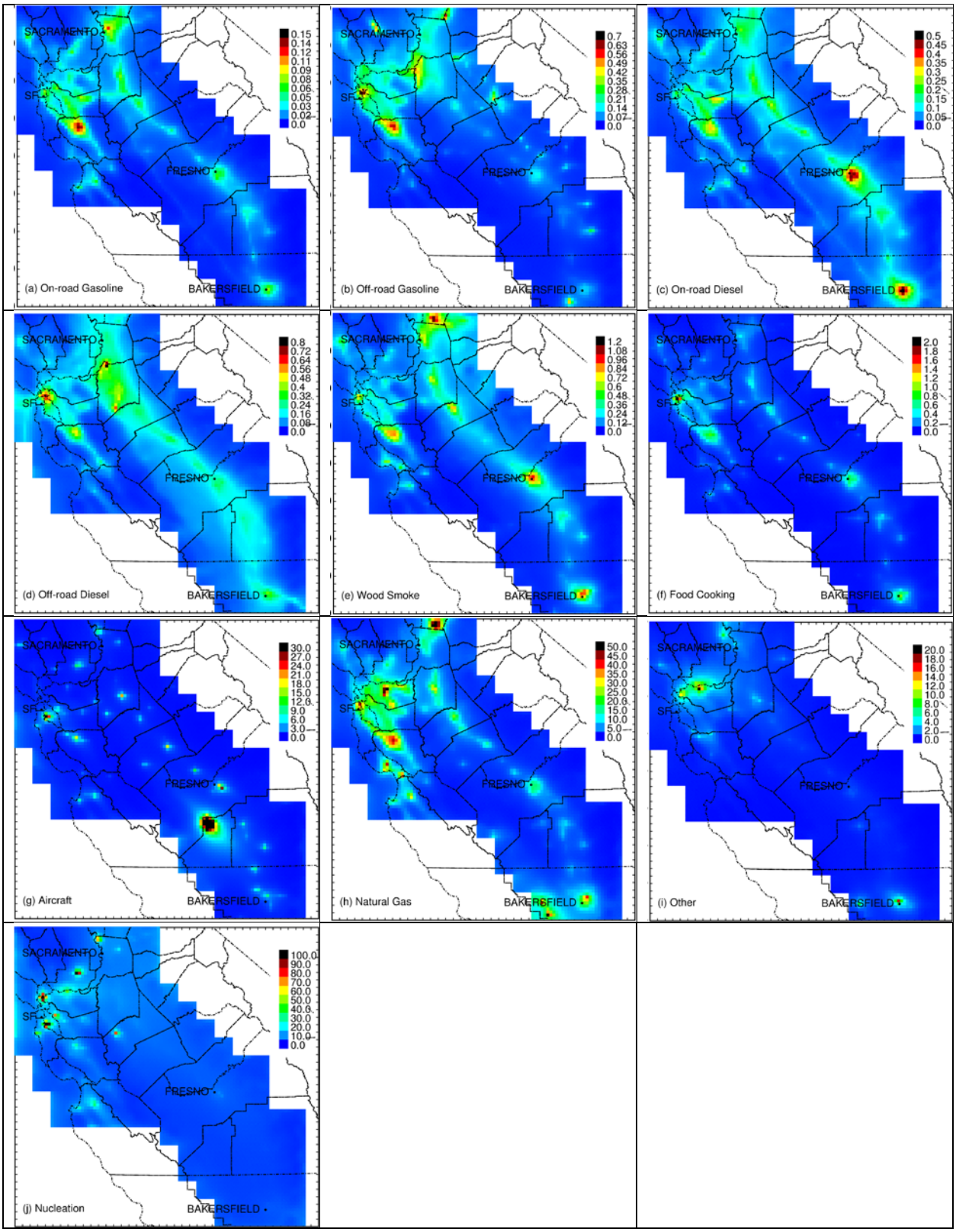

Figure 5. Spatial distribution of particle number from major sources in Northern California (unit: kcount/cm3).

Lines 524-526 have been updated to clarify that the diurnal variation of the natural gas combustion emissions noted by the reviewer were obtained independently from the emissions inventory specified by the California Air Resources Board. The activity pattern is based on energy demand as a function of time of day. Both natural gas combustion and motor vehicle activity follow the diurnal cycle of human activity across California, with peaks in the early morning and late afternoon. The current model predictions suggest that natural gas combustion contributes strongly to this pattern.

We acknowledge that the model predictions match the measured particle trends at some locations but not as well in other locations. We are not claiming that the model is perfect, but we feel that the information available does suggest that natural gas combustion is a major regional source of ultrafine particles that has not been previously recognized.

Reviewer 1 Comment 3: Modeling of growth of ultrafine particles. The approach used to simulate conden- sation/evaporation of sulfuric acid, ammonium, nitric acid, secondary organics on the ultrafine particles in this study is not explained in any detail. There is a rather confusing statement in lines 129-137 that "dynamic condensation/evaporation is not considered". Does this mean that the particles are assumed to be in equilibrium? If yes, how does the model deal with the effect of surface tension on the equilibrium vapor pressure es- pecially in the 10-20 nm range? Do these particles evaporate because their equilibrium vapor pressure is higher than that of the bigger particles? This is a crucial process for the number concentration of the smaller particles and it is not clear that it is simulated properly.

Response: Dynamic simulation of the condensation/evaporation of ultrafine particles is a computationally expensive exercise (Zhang et al. 2004, 2005; Zhang and Wexler 2004). Some of the particles evaporate downwind of sources like freeways, while other particles grow due to the condensation mostly of secondary organic aerosol (Anttila and Kerminen 2003; Troestl et al. 2016). The most extreme changes to the particle size distribution occur within the first few min after emissions to the atmosphere (within 300 m of roadways), with more stable behavior over long time periods.

Regional grid models used to predict regional number concentrations are not well-suited to simulating the dynamic behavior of the near-source particle size distribution for the first few minutes after release to the atmosphere. Evaporation of UFPs near the source is therefore represented by reducing the primary emissions of nano-particles based on measurements conducted at high dilution factors (Xue et al. 2018) or using measurements of particle volatility to estimate the evaporation at high dilution factors (May, Levin, et al. 2013; May, Presto, et al. 2013; Kuwayama et al. 2015). These regionally-representative emissions provide the starting point for the model calculations.

These points have been clarified on lines 159-175 of the updated manuscript.

The condensation of fresh sulfate, nitrate, ammonium ion, and SOA onto UFPs with diameters between 10 – 100 nm was simulated using the standard dynamic gas-particle partitioning methods in the model. These calculations do not change the predicted number concentration in the regional atmosphere. Condensation shifts the size distribution upward at a rate of approximately 2-3 nm hr^{-1} under favorable conditions. This has been clarified on lines 158-159 in the revised manuscript.

Reviewer 2 Comment 1: Definition of particle number concentration. The use of the term particle number concentration throughout this paper is often confusing and sometimes misleading. It is important to always define the lower threshold of the size range of the corresponding concentration. The total particle concentration can be easily a factor of 2 or 3 higher than the concentration of particles with diameter higher than 10 nm (N10).

Response: We will revise the paper to use the term N_x throughout where X refers to the lower size cut of the measurements or model predictions. The term PNC will no longer be used.

Reviewer 2 Comment 2: Growth of freshly nucleated particles to 10 nm. The authors state that they parameterize the growth process following the work of Kerminen and Kulmala (2002). However, this parameterization requires the growth rate (GR) of the particles. The calculation of this rate is non-trivial in a model with coarse aerosol size resolution such as the current one. Errors in the GR can lead to significant errors in the estimation of the contribution of nucleation as a source to particle number. The authors should evaluate the error of this parameterization for their aerosol model.

Response: The text on lines 104-129 and Figure 1 in the revised manuscript have been added to address this point. The growth rate (GR) in the Kerminen and Kulmala (2002) parameterization is one of the factors that accounts for the competition between the condensation and nucleation of over-saturated compounds until the nucleated particles grow to the size of the smallest bin in the regional model at which point this competition is represented explicitly by the model operators. In current study, we predicted the growth of the sulfate particles from nuclei using the equation

$$GR \approx \frac{3\times10^{-9}}{\rho_{nuc}} M_{sulf} u_{sulf} C_{sulf} \quad \text{(eq. 1)}$$

following (Kerminen and Kulmala 2002). Here, ρnuc is the density of the nucleation mode sulfate particles which was set to be 1.77 kg m-3 at 20°C, 1 atm; M_{sulf} is the molecular weight of nucleation mode sulfate particle which was set to be 98 g mol^{-1}; Csulf is the vapor concentration of sulfate (H_2SO_4); and u_{sulf} is temperature (T) dependent molecular speed of the sulfate vapor which is calculated as follows, in m s^{-1}.

$$u_{sulf} = \sqrt{\frac{8RT}{M_{sulf}}} \quad \text{(eq.2)}$$

According to (Kerminen and Kulmala 2002), uncertainty associated with eq. 1 is minor. Perturbation studies were conducted in the current analysis with a box model configured to represent a single grid cell using the full set of model operators. The GR predicted by eq 1 was multiplied by a factor ranging from 0.5 to 2.0 to test the sensitivity of the model results. Initial conditions were 0.04 ppm O_3, 0.05 ppm NO, 0.0 ppm NO_2, 0.05 ppm HCHO, 0.1 ppm ISOPRENE, 0.1 ppm BENZENE, and 0.01 ppm ALK5. A nucleation event was initiated at 8am by setting H_2SO_4 concentrations to 1e7 molecules cm^{-3} and NH_3 concentrations to 100 ppt. Figure 6 illustrates the growth of nucleated particles between 5am and 12 noon for July in California. The number concentration of nucleated particles increases to values between 2500 - 3000 #/cm3. SOA condenses on the particles causing their size to increase above 100nm. Coagulation and deposition processes remove particles over time.

Three separate simulations are illustrated in Figure 6 using the nominal GR predicted by eq 1 along with perturbations of 0.5*GR and 2.0*GR. These model perturbations fall almost exactly on top of the basecase simulations, suggesting that results are not overly sensitive to GR during the first few seconds of nuclei growth before calculations are handed off to the regional model algorithms.

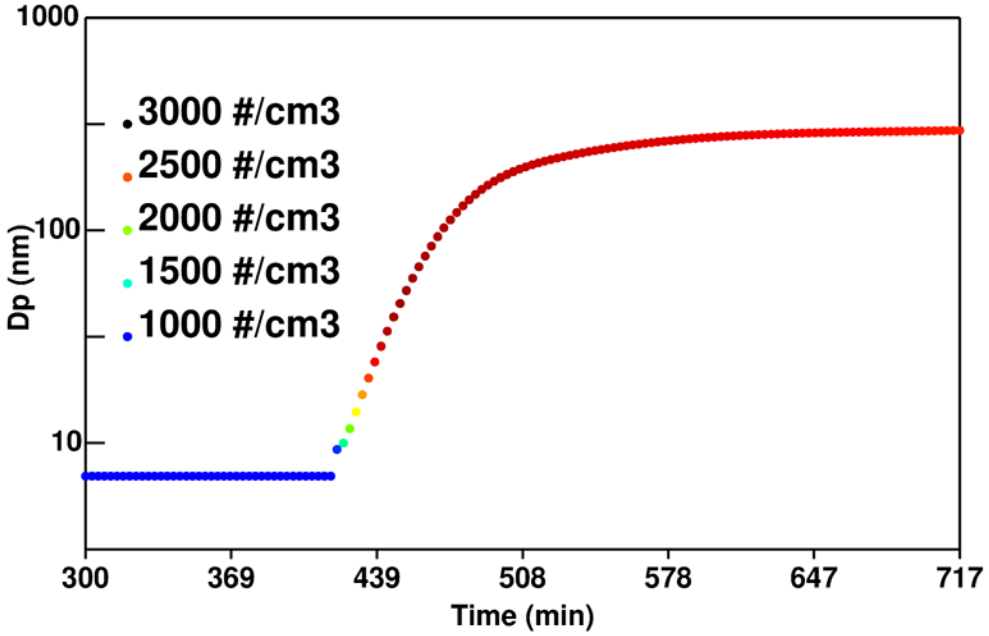

Fig 6: Simulated particle nucleation event followed by growth due to SOA condensation under conditions representing July in California. Vertical axis displays the mean diameter of the nuclei mode while color represents the particle number concentration.

Reviewer 2 Comment 3: There is little information provided about the frequency and spatial extent of nucleation in the simulations in the various seasons. This information is needed to under- stand the simulation results.

Response: The text on lines 595-620 in the revised manuscript have been added to address this point and the discussion is repeated below. The concentrations of nucleated particles in August, October, and December are shown in Figure 7 (Southern California) and Figure 8 (Northern California) below. Nucleation events occur in the regions where sulfur emissions are highest (typically airports, shipping ports and refining facilities). Concentrations of nucleated particles are higher in October and December than in August because colder temperatures increase nucleation rates if the precursor H_2SO_4 and NH_3 concentrations are relatively constant. A significant fraction of the H_2SO_4 in the current simulation is produced by the fast conversion of gas-phase SO_3 emissions to H_2SO_4 in the exhaust plume near the emissions source. SO_3 conversion does not depend on the presence of oxidants in the atmosphere and so the higher oxidant concentrations in the summer do not dominate the seasonal nucleation pattern.

Once H_2SO_4 forms in the exhaust plumes, it either condenses onto existing particles formed from lower volatility compounds in the plume, or it mixes with NH_3 in the background air and nucleates. This process is captured by dilution source sampling measurements that allow for a few minutes of aging time and so the size-resolved emissions profiles for many sources already account for the effects of nucleation within the “near-field” exhaust plume (within a few 10’s of meters after emission). SO_3 emissions from reciprocating internal combustion engines were therefore set to zero to avoid double

counting the new particle formation downwind of these sources in the current study. Regular SO_2 emissions from these sources were not modified. Emissions from aircraft jet engines have high exit velocity which promotes rapid mixing with background air. SO_3 emissions were left at their nominal levels (3-4% of total SOx) for jet engine aircraft in the current study. The consequence of these model treatments is that predicted concentrations of nucleated particles are highest downwind of LAX, which agrees with measurements of ambient particle number concentrations (Hudda et al., 2014).

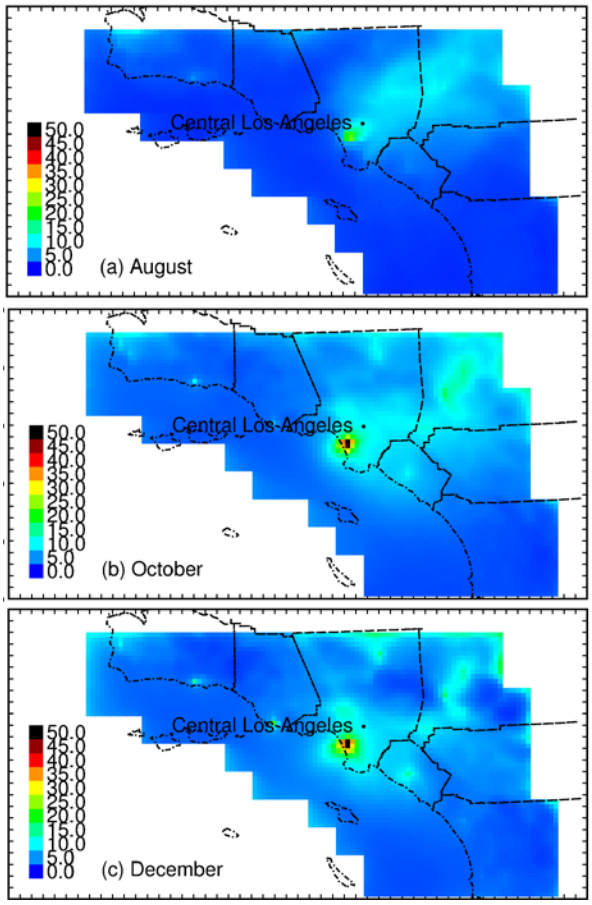

Figure 7: Seasonal variation of nucleated particle concentrations in Southern California. Units are kcount/cm^3.

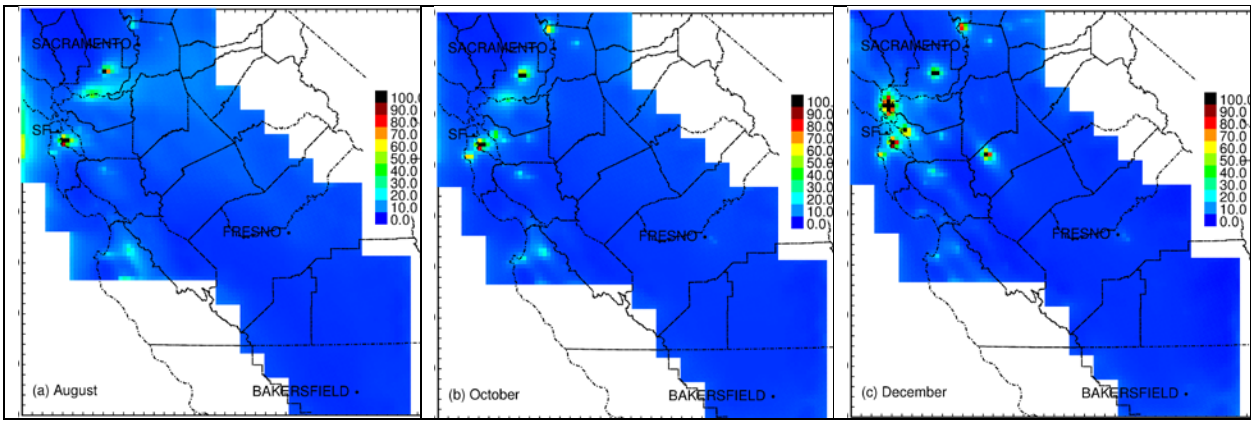

Figure 8: Seasonal variation of nucleated particle concentrations in Northern California. Units are kcount/cm^3.

Reviewer 2 Comment 4: Emissions from natural gas combustion. A map of the estimated N10 and PM0.1 emissions from this major source is needed (see also comment 1.2). Also the average diurnal profile of the emissions for the domain and the average size distribution should be shown.

Response: The map of emissions from natural gas sources are shown below and now included in the SI along with the diurnal profile of the natural gas emissions. Note that particulate matter emissions from all natural gas sources other than reciprocating engines have been reduced by 70% to account for evaporation of particles after emission to the atmosphere (Xue et al. 2018). The average diurnal profile of the natural gas emissions for the domain is shown in Figure S2 and the average size distribution is shown in Figure S3 of the original manuscript.

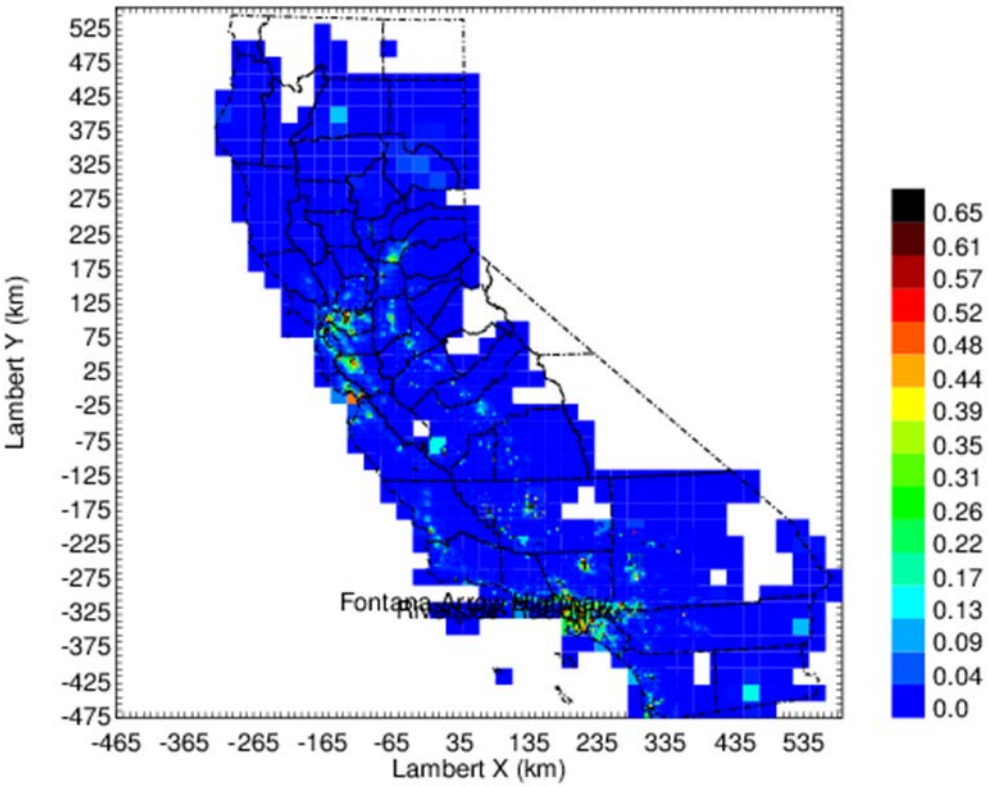

Figure 5. Daily average natural gas combustion emissions for California.

Reviewer 2 Comment 5: Temporal scale of evaluation. The authors present metrics of the model performance but they do not clarify if these are for hourly, daily, monthly, simulation averages or something else. The text and the corresponding tables do not include this information. Given the availability hourly measurements evaluation at this timescale should be also performed (if it has not been performed yet). The evaluation at a daily scale is also useful.

Response: Comparisons in the manuscript are based on daily averages which corresponds to the shortest averaging time that should be used for the current model results. Comparisons to measurements at hourly and daily time scales are shown in Figure 6 below for particle number concentration. The hourly comparisons meet model performance criteria, but have slightly worse performance than the daily averages because the calculations do not fully capture all of the random variability in meteorological patterns and emissions patterns over hourly time scales. Further work would be required to create accurate model results at hourly time scales, but this effort is beyond the reasonable scope of the current study. We do not wish to present hourly-average performance metrics in the manuscript because we do not want to encourage the use of the model results at this time scale.

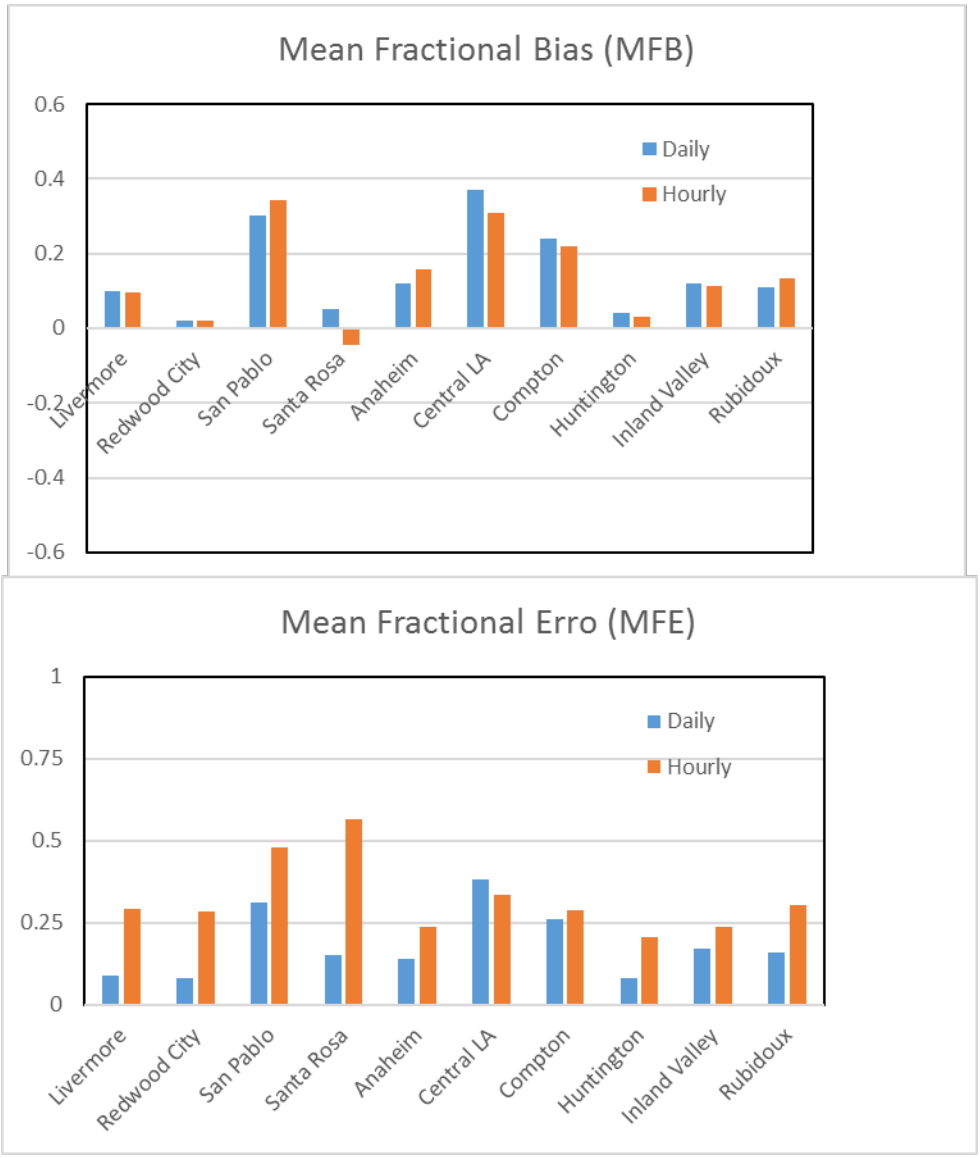

Figure 6 Mean Fractional Bias (MFB) and Mean Fractional Error (MFE) of "best-fit" N10 at 10 sites in California

Reviewer 2 Comment 6: The measurements of particle number refer to N6 and N7 while the predictions to N10. The authors suggest that the average error in the corresponding comparisons should be less than 10

Response: Yes, we feel that comparison between N6 to N10 will only introduce a small amount of uncertainty into the calculation. We would welcome recommendation from the reviewer to adjust the comparison to account for this size difference.

Reviewer 2 Comment 7: The use of qualitative terms (general agreement, agree reasonably well, good agreement) is not helpful and should be avoided.

Response: All qualitative statements have been removed in the final paper.

Reviewer 2 Comment 8: If my understanding of the paper is correct, the current model does not use the dynamic organic aerosol scheme used by Hu et al. (2017). If this is the case, the results regarding the contribution of SOA to PM0.1 in this work should be discussed and should be compared to that version of the model. If it is the same it should be clearly stated.

Response: We apologize that the original text was not clearer. The current study uses the same dynamic organic aerosol scheme used by (Hu et al. 2017). This point has been clarified on lines 158-159 in the revised manuscript.

Reviewer 2 Comment 9: Contribution of traffic particles. Ronkko et al. (PNAS, 114, 7549-7554, 2017) argued that traffic is an even more important source of particle number, because there are a lot of sub-10 nm particles emitted. Given that the current study does not include primary traffic particles smaller than 10 nm (which of course can grow to larger sizes), can it seriously underestimate the contribution of this source in urban environments?

Response: The measurements in the roadside environment consistently show that traffic dominates nano-particle concentrations. But the measurements moving downwind of the roadside environment show that these traffic nano-particles evaporate and do not increase the urban particle number concentration at distances more than 300 m downwind of the roadway (Zhu, Hinds, Kim, Shen, et al. 2002; Zhu, Hinds, Kim, and Sioutas 2002). This is a measurement conclusion based on independent work not associated with the current manuscript, but it supports the methods used to represent traffic in the regional calculations. These points have been clarified on lines 371-374 in the revised manuscript.

Reviewer 3 Comment 1: The abstract says that simulations have been performed for 2012, 2015 and 2016. However, the presented results are only for 2012. This is important because there are available size distribution measurements for 2015-16 in the modeling domain that can be used for the evaluation of the model predictions (see comment 1.2).

Response: Figures 2 and 3 show the results of the model predictions to CMB results for 2015 and 2016. These findings were added to show that the predictions for $PM_{0.1}$ traffic contributions are in good agreement with measurements, supporting the accuracy of the predictions for the relative importance of traffic vs. other sources of UFP.

The additional particle number concentration measurements in 2015-16 that could be added to the manuscript are the same type as those shown for 2012. All the number count measurements are for sites in the San Francisco Bay Area and Southern California that show essentially the same picture as the plots already included in the manuscript. A separate manuscript is under preparation showing comparisons to all available measurements from 2000-2016. We would like to present the full set of comparisons in a single manuscript rather than further fragmenting this dataset.

Reviewer 3 Comment 2: The predicted correlations between PM2.5 and particle number concentrations can be compared with the corresponding measured correlations as an indirect way to evaluate the model performance.

Response: Table3 below summarizes the predicted correlations between daily-average particle number concentrations and PM2.5 along with the measured correlations for these metrics. Measured correlations (R^2) are less than 0.25 at all locations except Santa Rosa where correlations are above 0.5. Model predictions for daily-average particle number concentrations and PM2.5 are more highly

correlated, with R^2 ranging from 0.22 to 0.73. Locations with high R^2 values such as central Los Angeles also have the highest MFB and MFE and so the high correlation between particle number and $PM_{2.5}$ may reflect inaccuracies in the model inputs. At other locations where traditional model performance metrics suggest that predictions are more accurate, the high correlation between particle number and $PM_{2.5}$ may be related to the model grid resolution. The 4km grid resolution used in the calculations smooths the sharp spatial gradients in the ultrafine particle concentration fields (see Response Figure 3). This same issue makes it difficult for point source measurements to accurately represent 4km average number concentrations. The particle number concentrations measured at a fixed monitoring location may not represent the variation in particle number concentrations a few km away. $PM_{2.5}$ concentration gradients are smoother, making model predictions and point measurements easier to compare. This analysis suggests that the model results contained in the current manuscript identify several important sources of ultrafine particles, but more work will be required to fully evaluate these results and possibly further refine the population exposure calculations.

Table 3. Daily-average correlation (R^2) between PM2.5 mass and particle number concentration at 8 sites in California.

R^2	Livermore	Redwood City	San Pablo	Santa Rosa	Anaheim	Central LA	Compton	Rubidoux
Obs	0.04	0.01	0.16	0.58	0.08	0.14	0.15	0.22
Sim	0.28	0.49	0.55	0.22	0.51	0.73	0.61	0.50

The points above have been added at lines 289-305 along with Table 2 in the revised manuscript.

Reviewer 3 Comment 3: Lines 66-67 “when nucleation algorithms were not standardized”. This statement is confusing.

Response: Will be changed to “…when different nucleation algorithms were used”.

Reviewer 3 Comment 4: Are the sulfate and nitrate concentrations shown in Table S4 for PM2.5 or for another size range?

Response: PM2.5

Reviewer 3 Comment 5: Table 1 should probably also include the predicted and measured average number concentrations.

Response: Revised Table 1 shown below and in revised manuscript.

	Ave Obs. Particles cm-3	Ave Sim. Particles cm-3	MFB	MFE	RMSE Particles cm-3

Livermore	8219	9201	0.10	0.09	3615
Redwood city	11500	11325	0.02	0.08	1132
San Pablo	10481	15822	0.30	0.31	10302
Santa Rosa	8655	8967	0.05	0.15	2063
Anaheim	12850	14812	0.12	0.14	4239
Central LA	17378	25376	0.37	0.38	10328
Compton	16203	21036	0.24	0.26	8127
Huntington	23207	24103	0.04	0.08	3698
Inland-Valley	15028	16875	0.12	0.17	4290
Rubidoux	10728	11920	0.11	0.16	3069

Reviewer 3 Comment 6: The terms “measured” and “predicted” should be used everywhere in Section 3.2.1 and other parts of the paper in which predictions are compared to measurements.

Response: This change will be made as suggested to the degree possible, but the term “measured” is too simplistic. The molecular marker measurements feed into a model prediction using the Chemical Mass Balance (CMB) model that has many model inputs and assumptions. There are no direct measurements of source contributions to PM0.1 – just model predictions using different techniques.

Reviewer 3 Comment 7: The number of samples and their duration corresponding to the results of Figs. 2-3 should be stated in the caption.

Response: Monthly average samples constructed from 3-day average measurements. This information has been added to figure caption as requested.

Reviewer 3 Comment 8: Line 296. Figures 4-6 and 7-9 do not show the seasonal variation of the corresponding variables. They show data (are these daily averages or something else) for different days in different seasons. These figures could be improved if they were split in four parts for the different periods simulated. The discussion could also be improved if the actual seasonal averages were shown (may be in the SI) and discussed.

Response: Figures show daily variation over months that span multiple seasons. The x-axis on each Figure has been improved to show the months more clearly. Figure captions have been expanded to better explain the results.

Reviewer 3 Comment 9: Figure S2. What is A, B, and C? What is the average pattern in the domain?

Response: A, B and C represent different diurnal profiles used for different natural gas sources or regions based on information supplied by the California Air Resources Board. The average diurnal profile has been added to Figure S2.

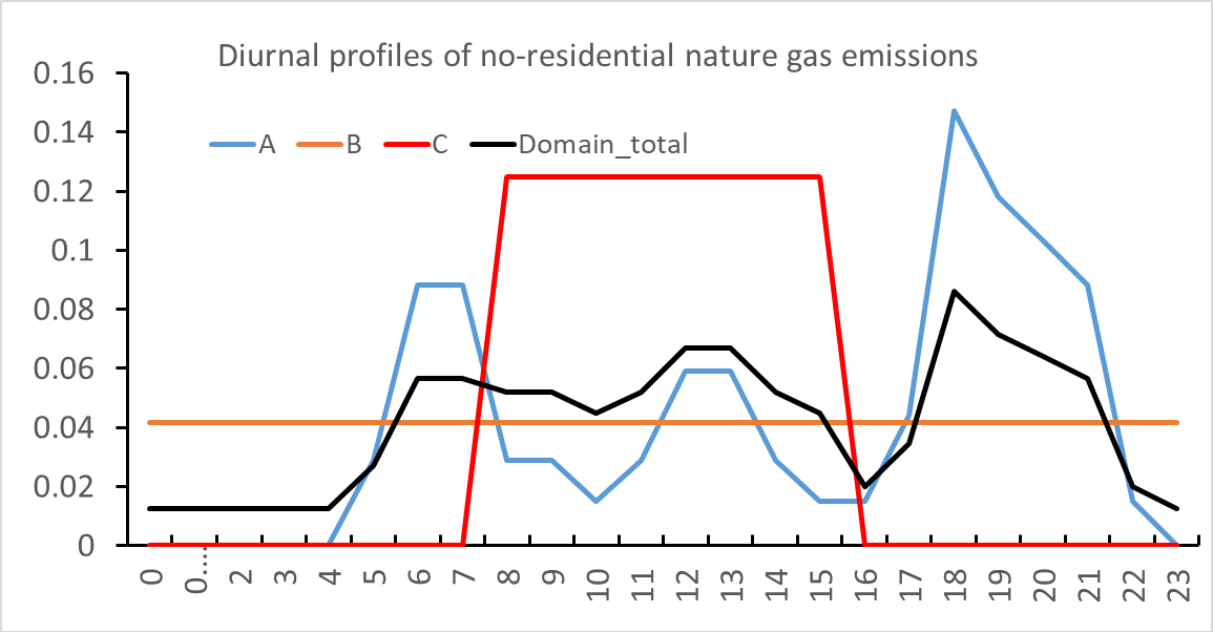

Figure S2 Diurnal profiles of no-residential natural gas emissions. A, B and C represents different types of diurnal profiles applied to natural gas emissions in the model. Black curve represents the average pattern in the domain.

References

Hudda, N., Gould, T., Hartin, K., Larson, T. V., and Fruin, S. A.: Emissions from an International Airport Increase Particle Number Concentrations 4-fold at 10 km Downwind, Environmental science & technology, 48, 6628-6635, 10.1021/es5001566, 2014.

Zhang, K. M., Wexler, A. S., Zhu, Y. F., Hinds, W. C., and Sioutas, C.: Evolution of particle number distribution near roadways. Part II: the 'road-to-ambient' process, Atmospheric Environment, 38, 6655-6665, 10.1016/j.atmosenv.2004.06.044, 2004.

Zhang, K. M., Wexler, A. S., Niemeier, D. A., Zhu, Y. F., Hinds, W. C., and Sioutas, C.: Evolution of particle number distribution near roadways. Part III: Traffic analysis and on-road size resolved particulate emission factors, Atmospheric Environment, 39, 4155-4166, 10.1016/j.atmosenv.2005.04.003, 2005.

Zhu, Y. F., Hinds, W. C., Kim, S., Shen, S., and Sioutas, C.: Study of ultrafine particles near a major highway with heavy-duty diesel traffic, Atmospheric Environment, 36, 4323-4335, 10.1016/s1352-2310(02)00354-0, 2002a.

Zhu, Y. F., Hinds, W. C., Kim, S., and Sioutas, C.: Concentration and size distribution of ultrafine particles near a major highway, Journal of the Air & Waste Management Association, 52, 1032-1042, 10.1080/10473289.2002.10470842, 2002b.

Regional Sources of Airborne Ultrafine Particle Number and Mass Concentrations in California

Xin Yu[1], Melissa Venecek[2], Anikender Kumar[1], Jianlin Hu[3], Saffet Tanrikulu[4], Su-Tzai Soon[4], Cuong Tran[4], David Fairley[4], and Michael J. Kleeman[1]*

[1]Department of Civil and Environmental Engineering, University of California, Davis. One Shields Avenue, Davis CA. [2]Department of Land, Air, and Water Resources, University of California, Davis. One Shields Avenue, Davis CA. [3]School of Environmental Science and Engineering, Nanjing University of Information Science and Technology. [4] Bay Area Air Quality Management District, San Francisco, CA.

*Corresponding author. Tel.: +1 530 752 8386; fax; +1 530 752 7872. E-mail address: mjkleeman@ucdavis.edu (M.J. Kleeman).

Abstract

Regional concentrations and source contributions are calculated for airborne particle number concentration (~~PNC~~N_x) and ultrafine particle mass concentration ($PM_{0.1}$) in the San Francisco Bay Area (SFBA) and the South Coast Air Basin (SoCAB) surrounding Los Angeles with 4 km spatial resolution and daily time resolution for selected months in the years 2012, 2015, and 2016. Performance statistics for daily predictions of ~~PNC~~ N_{10} concentrations meet the goals typically used ~~threshold normally required~~ for ~~regulatory~~ modeling of $PM_{2.5}$ (MFB< ± 0.5 and MFE < 0.75). The relative ranking and concentration range of ~~Predicted~~ source contributions to $PM_{0.1}$ predicted by regional calculations agree ~~are in good agreement~~ with results from receptor-based studies that use molecular markers for source apportionment at four locations in California. Different sources dominated regional concentrations of ~~PNC~~ N_{10} and $PM_{0.1}$ because of the different emitted particle size distributions and different choices for heating fuels. Nucleation (24-57%) ~~Non-residential natural gas combustion (38-74%)~~ made the largest single contribution to ~~PNC~~ N_{10} concentrations at the ten regional monitoring locations, followed by natural gas combustion (28-45%), ~~nucleation (6-14%),~~ aircraft (2-10%), mobile sources (1-5%), ~~wood smoke (1-8%),~~ food cooking (1-29%), and ~~mobile sources~~wood smoke (0-1%~~4-8%~~). In contrast, natural gas combustion ~~wood smoke~~ (225-5249%) was the largest source of $PM_{0.1}$ ~~in the SFBA~~ followed by mobile sources (1515-33-42%), ~~non-~~

~~residential natural gas combustion (13-28%), and~~ food cooking (4%-14%), wood combustion (1-12%), and aircraft (2-6%). ~~Non-residential natural gas combustion (42-57%) was the largest $PM_{0.1}$ source at the SoCAB sites, followed by traffic sources (16-35%) and food cooking (6-14%).~~ The study region encompassed in this project is home to more than 25M residents, which should provide sufficient power for future epidemiological studies on the health effects of airborne ultrafine particles. ~~Correlations between $PM_{2.5}$ and PNC are low (R^2=0.35) suggesting that the health effects of these metrics may be assessed independently.~~ All of the $PM_{0.1}$ and ~~PNC~~ N_{10} outdoor exposure fields produced in the current study are available free of charge at http://webwolf.engr.ucdavis.edu/data/soa_v2/monthly_avg2.

1. Introduction

Numerous epidemiological studies have identified positive correlations between exposure to ambient particulate matter (PM) and increased risk of respiratory and cardiovascular diseases, premature mortality and hospitalization (Pope et al., 2002;Pope et al., 2004;Pope et al., 2009;Dockery and Stone, 2007;Ostro et al., 2015;Ostro et al., 2006;Ostro et al., 2010;Brunekreef and Forsberg, 2005;Fann et al., 2012;Gauderman et al., 2015;Miller et al., 2007). Most of these studies have not fully addressed ultrafine particles (UFPs; Dp<0.1µm) because these particles make a very small contribution to total ambient PM mass (Ogulei et al., 2007). Toxicity studies suggest that UFPs may be especially dangerous to human health since they have higher toxicity per unit mass (Li et al., 2003;Nel et al., 2006;Oberdorster et al., 2002) and can penatrate the lungs and enter the bloodstream and secondary organs (Sioutas et al., 2005). These toxicology results are suggestive but more epidemiological evidence is required before the threat to public health from UFPs can be fully assessed.

Most previous UFP epidemiology studies are based on particle number concentration (~~P~~N_{x} – the number of particles with diameter less than X nm) measured at fixed sites using commercially-available instruments. These devices are expensive and they require regular maintence which limits the number of measurement sites that can be deployed.

Formatted: Subscript

Translating measured ~~P~~N_{x}~~C~~ into population exposure estimates is also difficult because UFP concentrations change more rapidly over shorter distances than $PM_{2.5}$ (Hu et al., 2014b;Hu et al., 2015;Hu et al., 2014a). Land use regression (LUR) models could potentially be used to interpolate UFP concentrations between sparse measurement locations, but the atmospheric processes governing ~~PNC~~N_x concentrations are highly non-linear and (so far) sufficient training data is not generally available for LUR models to estimate ~~PNC~~N_x exposure over a large enough population to support a definitive epidemiology study (Montagne et al., 2015). Previous attempts to use regional reactive chemical transport models to predict ~~PNC~~N_x in highly populated regions have focused on nucleation, yieldeding a wide range of predicted concentrations and only modest agreement with measurements when different nucleation algorithms were used~~not standardized~~ (Elleman and Covert, 2009b;Zhang et al., 2010;Elleman and Covert, 2009a). Obtaining accurate exposure estimates to ~~PNC~~N_x in highly populated regions therefore remains a major challenge in UFP epidemiological studies.

Recent work has examined UFP mass ($PM_{0.1}$) as an alternative metric for UFP exposure, and demonstrated that $PM_{0.1}$ can be predicted with reasonable accuracy over large populations using regional reactive chemical transport models (Hu et al., 2014b;Hu et al., 2014a). The $PM_{0.1}$ exposure fields developed using this technique have been used in multiple epidemiological studies that revealed associations with mortality and pre-term birth (Ostro et al., 2015;Laurent et al., 2016). Despite the success of studies using $PM_{0.1}$, techniques that estimate ~~PNC~~ N_x exposure are still needed because a large number of ongoing UFP studies are based on ~~PNC~~N_x and it is possible that $PM_{0.1}$ and ~~PNC~~N_x are associated with different types of health effects.

Here we extend the previous work using regional reactive chemical transport models for UFPs to include ~~PNC~~N_x in the San Francisco Bay Area (SFBA) and the South Coast Air Basin (SoCAB) region around Los Angels which are the two most densely populated major metropolitan location in California. Source contributions to $PM_{0.1}$ and ~~PNC~~N_x are tracked using the University of California, Davis / California Institute of Technology (UCD/CIT) regional reactive chemical transport model with 4 km spatial resolution. Predicted concentrations during the year 2012 are compared to measurements available at

Formatted: Subscript

~~10~~ ten regional monitoring sites. The spatial distribution fields of different particle metrics (~~PNC~~N_x, $PM_{0.1}$, $PM_{2.5}$) are combined with population distributions to estimate exposure. To the best of our knowledge, this is the first integrated study of both UFP number and mass using a regional reactive chemical transport model in California.

Formatted: Subscript

2. Model Description

The UCD/CIT chemical transport model used in the current study has been succesfully applied in sevaral previous studies in the San Joaquin Valley (SJV) and the SoCAB (Ying et al., 2008b;Ying et al., 2008a;Hu et al., 2015;Hu et al., 2017;Chen et al., 2010;Held et al., 2004;Held et al., 2005;Hixson et al., 2010;Hixson et al., 2012;Hu et al., 2012;Kleeman and Cass, 2001;Kleeman et al., 2007;Kleeman et al., 1997;Mahmud, 2010;Mysliwiec and Kleeman, 2002;Rasmussen et al., 2013;Ying and Kleeman, 2006;Zhang and Ying, 2010). The model ~~It~~ includes algorithms for emissions, transport, dry deposition, wet deposition, gas phase chemistry, gas-to-particle conversion, coagulation, and some condensed phase chemical reactions. Nucleation was added to the model for the first time in the current study using the ternary nucleation (TN) mechanism involving H_2SO_4-H_2O-ammonia (NH_3) (Napari et al., 2002). As was the case in previous studies using this algorithm, the resulting nucleation rate was adjusted using a tunable nucleation parameter set to 10^{-5} for new particle nucleation (Jung et al., 2010). The Kerminen and Kulmala (2002) parameterization was added in order to bridge the gap between the 1 nm particle nuclei and their appearance into the smallest size bin of the UCD/CIT model (~10 nm). The nuclei growth rate (GR) in the Kerminen and Kulmala (2002) parameterization is one of the factors that accounts for the competition between the condensation and nucleation of over-saturated compounds until the nucleated particles grow to the size of the smallest bin in the regional model at which point this competition is represented explicitly by the model operators. In the current study, the GR for nucleated sulfate particles was calculated using the diffusion-limited condensation rate of sulfuric acid based on the recommendation of Kerminen and Kulmala. Once particles reach ~10nm, the full operators in the model calculations predict growth by condensation of sulfuric acid, nitric acid, ammonia, and secondary organic aerosol (SOA). Perturbation studies were conducted in the current analysis to test the effect of

GR with a box model configured to represent a single grid cell using the full set of model operators. Initial conditions in the SAPRC11 gas-phase mechanism were 0.04 ppm O_3, 0.05 ppm NO, 0.0 ppm NO_2, 0.05 ppm HCHO, 0.1 ppm ISOPRENE, 0.1 ppm BENZENE, and 0.01 ppm ALK5. A nucleation event was initiated at 8am by setting H_2SO_4 concentrations to 10^7 molecules cm^{-3} and NH_3 concentrations to 100 ppt. The nominal GR was multiplied by a factor ranging from 0.5 to 2.0 to test the sensitivity of the model results. Figure 1 illustrates the growth of nucleated particles between 5am and 12 noon for conditions representing July in California. The number concentration of nucleated particles increases from zero to values between 2500 - 3000 # cm^{-3}. SOA condenses on the particles causing their size to increase above 100nm. Coagulation and deposition processes remove particles over time. Three separate simulations are illustrated in Figure 1 using the nominal GR along with perturbations of 0.5*GR and 2.0*GR. These model perturbations fall almost exactly on top of the basecase simulations, suggesting that results are not overly sensitive to GR during the first few seconds of nuclei growth before calculations are handed off to the regional model algorithms.

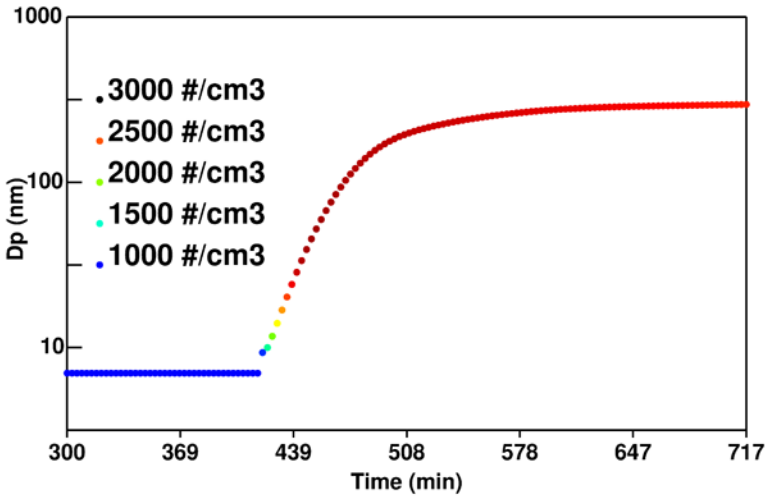

Figure 1: Simulated particle nucleation event followed by growth due to SOA condensation under conditions representing July in California. Vertical axis displays the

Formatted: Subscript
Formatted: Subscript
Formatted: Subscript
Formatted: Subscript
Formatted: Superscript
Formatted: Superscript
Formatted: Subscript
Formatted: Superscript

mean diameter of the nuclei mode while color represents the particle number concentration.

Several previous modeling studies have been conducted to evaluate the performance of the ternary nucleation mechanism on predicted ~~particle number concentration (PNC)~~N_x using global and regional models. Jung et al. (2010) found that a scaled version of the ternary H_2SO_4-NH_3-H_2O nucleation theory (Napari et al.,2002 with a supplemental 10^{-5} nucleation tuning factor) added to the PMCAMx-UF model produced ~~PNC~~N_x predictions in reasonable agreement with observations. The study of Westervelt et al. (2013) also showed that the ternary nucleation parameterization (with a supplemental 10^{-5} nucleation tuning factor) added to the Goddard Earth Observing System global chemical transport model (GEOS-Chem) produced reasonable ~~PNC~~ N_x predictions on average when compared with measurements at five locations spanning various environments. Jung et al. (2008) considered multiple nucleation parameterizations in the Dynamic Model for Aerosol Nucleation (DMAN) to predict the nucleation events and non-events observed during the Pittsburgh Pittsburgh Air Quality Study (PAQS) conducted between July 2001 and September 2002. Their results showed that the ternary nucleation mechanism ((Napari et al., 2002) with a supplemental 10^{-5} nucleation tuning factor) was a suitable nucleation scheme for 3-D chemical transport models. Although there have been numerous significant efforts to incorporate nucleation algorithms into three-dimensional regional and global models (Jung et al., 2008;Jung et al., 2010;Westervelt et al., 2013;Zhang et al., 2010), nucleation modeling studies are still in the early stages of development and further efforts are needed to reduce the uncertainty in both the nucleation rate and growth mechanisms.

In the current study, emission, transport, deposition, and coagulation of UFPs were simulated using operators developed for the UCD/CIT model framework, leading to modification of the particle size distribution and the subsequent ~~PNC~~ N_x concentrations. Dynamic condensation / evaporation is ~~is not~~ considered for all particle size bins with predicted UFP growth rates of 2-3 nm hr^{-1} or higher under favorable conditions. The regional model operators are not well suited for the most extreme changes to the particle size distribution that occur within the first few seconds or minutes after emissions to the

atmosphere (such as within 300 m of roadways). Dedicated simulations can predict the dynamic condensation/evaporation of particles at distances of 10's of meters downwind of the roadway (Zhang et al., 2005;Zhang et al., 2004) mostly due to the partitioning of SOA (Anttila and Kerminen, 2003;Trostl et al., 2016), but these calculations are too expensive for domains spanning thousands of km. Regional calculations such as those illustrated in the current study rely on emissions characterization measurements that include a few minutes of aging to capture the "near-field" emissions of particle size and composition that can then be used as the starting point for regional model calculations. In some cases, evaporation of UFPs in the first few seconds after release to the atmosphere is therefore represented by reducing the primary emissions of nano-particles based on measurements conducted at high dilution factors (Xue et al., 2018a) or using measurements of particle volatility to estimate the evaporation at high dilution factors (May et al., 2013a;May et al., 2013b;Kuwayama et al., 2015). ~~nucleation mode particles because these processes act slowly on the regional scale relative to the other operators and they do not strongly alter the ground-level PNC outside the near-roadway environment (within 300 m or major highways). This 0.3km resolution is beyond the scope of the current modeling exercidse which uses 4 km spatial resolution in the horizontal direction. Furthermore, the dynamic condensation / evaporation calculations are too expensive to track for nucleation mode particles in regional model applications.~~ All of the results presented in the current analysis ~~The model configuration in the current study reflects the~~ focus on regional UFP concentrations with 4km resolution~~, not near-roadway UFP concentrations~~.

The model domains used in the study are shown in Figure 2~~1~~. The parent domain with 24 km horizontal resolution covered the entire state of California (referred to as CA_24 km) and the two nested domains with 4 km horizontal resolution covered the SFBA + SJV + South Sacramento Valley air basins (referred as SJV_4 km) and the SoCAB surrounding Los Angeles (referred as SoCAB_4 km). The UCD/CIT model was configured with 16 vertical layers up to a height of 5 km above ground level, with 10 layers in the first 1 km. Previous studies have shown that this vertical configuration captures the air pollution system above California (Hu et al., 2014a;Hu et al., 2014b;Hu et al., 2015). Particulate number, mass, and composition are represented in 15 size bins, with particle diameters

being centered within equally spaced logarithmic size interval spanning the diameter range from 0.01 to 10µm. Nucleated particles were initialized in a 16th size bin with initial diameter of 0.01 µm.

Formatted: Superscript

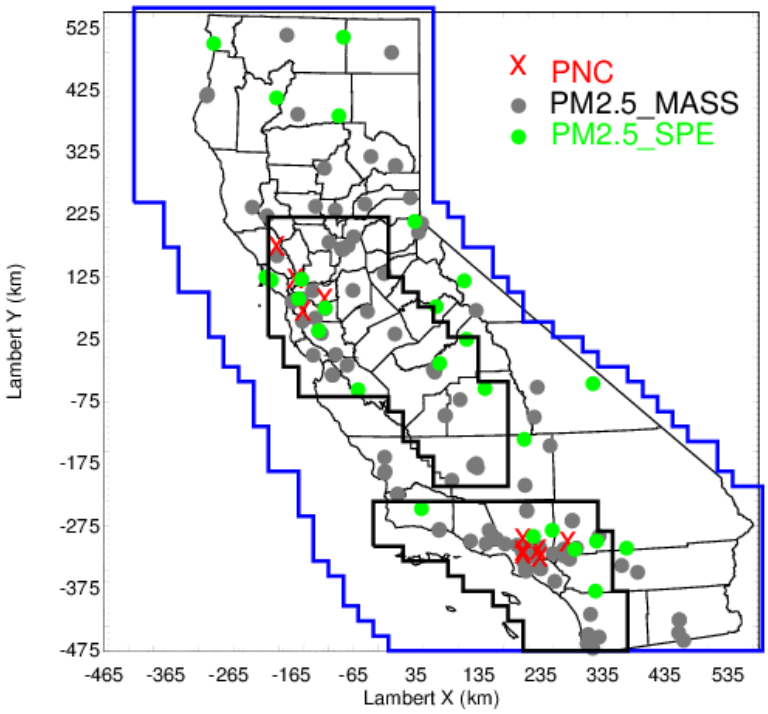

Figure 2~~1~~: Modeling domains. Blue lines outline the CA_24 km domain, black lines outline the SoCAB_4 km (bottom) and SJV_4 km domains (top). Red crosses represent ten ~~particle number concentration (PNC)~~N_x sites (fours sites operated by staff at the Bay Area Air Quality Management District (BAAQMD) and six sites from the Multiple Air Toxics Exposure Study IV (MATES IV)). Detailed location information for the ~~PNC~~ N_x sites is listed in Table S3. Green dots represent BAAQMD $PM_{2.5}$ speciation network sites and the Interagency Monitoring of Protected Visual Environments (IMPROVE) sites; gray dots represent the $PM_{2.5}$ federal reference method (FRM) sites.

2.1 Meteorological Fields

Hourly meteorological fields during the modeling period were generated by the Weather Research and Forecasting (WRF) model version 3.4 with three nested domains that had horizontal resolutions of 36 km, 12 km and 4 km, respectively. In the present simulations, the WRF model was configured with 50 vertical layers (up to 100 hpa) and four-

dimensional data assimilation (FDDA) nudging was utilized to improve the agreement between model predictions and observed meteorological patterns (Otte, 2008b, a). WRF predictions for wind speed, temperature, and relative humidity were compared to measurements for seven counties in the SFBA and two counties in SoCAB (see Table S2). Temperature has mean bias (MB) within ~0.2 ˚C and root- mean-square errors (RMSE) between 4-5 ˚C. Wind speed has mean fraction bias (MFB) within ±0.20 and RMSE generally <2.0 m/s. This level of performance is consistent with performance of WRF in previous studies conducted in California (Zhao et al., 2011;Hu et al., 2015).

2.2 Emissions

The emission inventories used in the SFBA were developed by the BAAQMD for the year 2012 based on the regulatory inventory provided by the California Air Resources Board for that same year. The SFBA inventory was processed using the Sparse Matrix Operator Kernel Emissions (SMOKE) v3.7 software package provided by US EPA. SMOKE was configured to separately tag emissions from on-road gasoline vehicles, off-road gasoline vehicles, on-road diesel vehicles, off-road diesel vehicles, food cooking, biomass burning, non-residential natural gas, and all other sources. The emission inventories used in South Sacramento Valley, SJV and SoCAB were provided by the California Air Resources Board.

Measurements conducted in parallel with the current study found that particles emitted from natural gas combustion in home appliances were semi-volatile when diluted by a factor of 25 in clean air, but particles emitted from reciprocating engines ~~industrial sources~~ did not evaporate under the same conditions (Xue et al., 2018a). Near-field emissions from all ~~residential~~ natural gas sources combustion sources other than reciprocating engines were therefore set to 30% of ~~zero in the current study while emissions from other natural gas combustion sources were retained at~~ their nominal levels. A map of the natural gas emissions distribution is shown in Supporting Information (Figure S3).

SMOKE results were transformed into size-resolved emissions of particle number, mass, and composition using measured source profiles through an updated version of the emissions model described by Kleeman and Cass (1998). The PM profiles used for each source type were specified as weighted averages from each of the detailed sources within each broad category as summarized in Table S1. Detailed PM source profiles for major sources of ultrafine particulate matter are based on measurements conducted during source tests (Li and Hopke, 1993;Kleeman et al., 1999, 2000;Robert et al., 2007a;Robert et al., 2007b;Mazaheri et al., 2009). In most cases, these emissions size distributions strongly influence the size distributions of particles in the ambient atmosphere (see Figures S1 and S~~3~~4). A more detailed discussion of the emissions processing has been presented in a previous study (Hu et al., 2015).

3. Results

3.1 Statistical Evaluation

According to Taylor's Hypothesis (Shet et al., 2017), it is expected that the spatial distribution of model results is more important than the temporal distribution when evaluating performance. In the current study model performance evaluations are limited to the locations where measurements were made. Therefore, the temporal distribution is also considered by comparing predicted vs. measured daily average ~~PNC~~ N_x, $PM_{2.5}$ and individual $PM_{2.5}$ species mass concentrations.

The evaluation data set was compiled from several measurement networks including the sites operated by staff at the Bay Area Air Quality Management District (BAAQMD), the IMPROVE sites, the MATES IV sites and FRM sites. In ~~recognition~~order to account for ~~of~~ the uncertainty in predicted wind fields and spatial surrogates used to place emissions, "best-fit" model results were created by identifying the closest match within 3 grid cells of each measurement location. "Best-fit" m~~M~~odel performance for $PM_{2.5}$ at routine monitoring sites (~~Figure 1~~Figure 2) ~~generally~~ meets the performance criteria suggest by Boylan and Russell (Boylan and Russell, 2006) (mean fractional error (MFE) ≤ +0.75 and mean fractional bias (MFB) ≤ ±0.5) (Table S4). Table S5 shows the MFB and MFE values of gaseous species of O_3, NO, NO_2, CO and SO_2 using daily averages across all measurement sites during the entire simulated period. Gaseous species of O_3, CO, NO, NO_2 and SO_2 have MFBs within ± 0.3 and MFE less than 0.5, indicating consistent behavior ~~general agreement~~ between predictions and measurement for these species. The ability of UCD/CIT predictions for key gas species, mass and chemical component concentrations in the $PM_{0.1}$ and $PM_{2.5}$ size fractions was also evaluated in previous studies (Ying and Kleeman, 2006;Ying et al., 2008a;Ying et al., 2008b;Hu et al., 2012;Chen et al., 2010;Held et al., 2005;Hu et al., 2015;Hu et al., 2017;Venecek et al., 2018). The performance of the UCD/CIT air quality model in these studies generally meets standard model performance criteria. Of greatest interest in the current study, predicted "best-fit" ~~PNC~~ N_{10} values were compared to measured $N_{7\text{-}1000}$ ~~(aerosol number concentrations for particle diameters ranging from 7nm-1000nm)~~ values at four sites in the SFBA (Santa Rosa, San Pablo, Redwood City and Livermore) and six sites in SoCAB (Anaheim, Central Los Angeles, Compton, Huntington, Inland-valley and Rubidoux). $N_{7\text{-}1000}$ measurements in the SFBA were made using an Environmental Particle Counter (EPC) Monitor Model 3783 (TSI Inc) while $N_{7\text{-}1000}$ measurements in the SoCAB were made with EPC Model 3781 (TSI Inc). Both monitors can detect ultrafine particles down to 7 nm which is smaller than the first size bin of 10 nm used in model calculations. Previous studies conducted at Fresno, California, suggest that $N_{7\text{-}10}$ accounts for approximately 8% of $N_{7\text{-}1000}$ (Watson et al., 2011), and so some amount of negative bias is expected when comparing predicted ~~PNC (=~~$N_{10\text{-}1000}$~~)~~ to measured $N_{7\text{-}1000}$. The evaluation results for "best-fit" ~~PNC~~N_{10} summarized in Table 1 follow this expected

trend but mean fractional bias (MFB) and mean fractional error (MFE) at each comparison site still meet the $PM_{2.5}$ performance criteria suggested by Boylan and Russell (2006). This level of performance is comparable to the results from a previous UFP number simulation conducted in Northern California using a modified version of the WRF-Chem model (Lupascu et al., 2015). The ~~good~~ level of agreement between predicted "best-fit" and measured $PM_{2.5}$, individual $PM_{2.5}$ species, key gas species and ~~PNC~~N_{10} builds confidence in the model skill for UFP predictions in the current study.

Table 1. Performance statistics for “best-fit” ~~PNC (=~~N_{10}~~-1000)~~ predictions vs. N_7 at individual monitoring sites. Threshold for ~~regulatory~~ PM modeling applications is typically MFB< ± 0.5 and MFE < 0.75.

	Ave Obs. Particles cm^{-3}	Ave Sim. Particles cm^{-3}	MFB	MFE	RMSE Particles/cm^{-3}
Livermore	8219	9201	0.10	0.09	3615
Redwood city	11500	11325	0.02	0.08	1132
San Pablo	10481	15822	0.30	0.31	10302
Santa Rosa	8655	8967	0.05	0.15	2063
Anaheim	12850	14812	0.12	0.14	4239
Central LA	17378	25376	0.37	0.38	10328
Compton	16203	21036	0.24	0.26	8127
Huntington	23207	24103	0.04	0.08	3698
Inland-Valley	15028	16875	0.12	0.17	4290
Rubidoux	10728	11920	0.11	0.16	3069

Table 2 below summarizes the predicted correlations between daily-average particle number concentrations and $PM_{2.5}$ along with the measured correlations for these metrics. Measured correlations (R^2) are less than 0.25 at all locations except Santa Rosa where correlations are above 0.5. Model predictions for daily-average particle number concentrations and $PM_{2.5}$ are more highly correlated, with R^2 ranging from 0.22 to 0.73. Locations with high R^2 values such as central Los Angeles also have the highest MFB and MFE and so the high correlation between particle number and $PM_{2.5}$ may reflect inaccuracies in the model inputs. At other locations where traditional model performance metrics suggest that predictions are more accurate, the high correlation between particle number and $PM_{2.5}$ may be related to the model grid resolution. The 4km grid resolution used in the calculations smooths the sharp spatial gradients in the ultrafine particle concentration fields (see Figure 4 below). This same issue makes it difficult for point source measurements to accurately represent 4km average number concentrations. The particle number concentrations measured at a fixed monitoring location may not

represent the variation in particle number concentrations a few km away. $PM_{2.5}$ concentration gradients are smoother, making model predictions and point measurements easier to compare.

Table 2. Daily-average correlation (R^2) between PM2.5 mass and particle number concentration at 8 sites in California.

R^2	Livermore	Redwood City	San Pablo	Santa Rosa	Anaheim	Central LA	Compton	Rubidoux
Obs	0.04	0.01	0.16	0.58	0.08	0.14	0.15	0.22
Sim	0.28	0.49	0.55	0.22	0.51	0.73	0.61	0.50

Formatted: Font: (Default) Times New Roman, 12 pt, Font color: Auto

Formatted: Font color: Auto

Formatted: Font color: Auto

Formatted: Font color: Auto

Formatted: Font color: Auto

3.2 $PM_{0.1}$ and ~~PNC~~ N_{10} Source Apportionment in California

The UCD/CIT model uses a moving sectional approach to conserve particle number and mass while letting particle radius change due to condensation and evaporation (Kleeman et al., 1997). The method to calculate source contributions to number concentration is performed for each moving section individually. Number is explicitly conserved and correctly apportioned to sources in this algorithm. Each particle source type / moving size bin includes an artificial tracer equal to 1% of the primary particle mass. The mass of this tracer is related to the number of particles by the equation

$$tracer\_source\_i * 100 = N\_source\_i * 3.14159/6 * Dp\_bin * \rho\_i \quad (eq1)$$

Formatted: Centered

where ρ_i is the density of primary particles emitted from source i. This equation can be easily rearranged to solve for N_source_i as a function of tracer_source_i in each size bin. Condensation/evaporation changes the particle diameter as semi-volatile components move on and off the particle but this does not change tracer_source_i or N_source_i. As a result, the moving sectional approach greatly simplifies the source apportionment of particle number compared to other models that use fixed particle size bins with condensation / evaporation transferring material between bins.

Coagulation complicates source apportionment calculations for particle number because coagulation events conserve particle mass but destroy particle number. The model

calculations treat the most frequently occurring coagulation events between very small particles and very large particles in a manner analogous to condensation. When two particles coagulate, the mass of the smaller particle is added to the mass of the larger particle. The number concentration of the smaller particle is discarded while the number concentration of the larger particle stays constant. This slightly reduces the accuracy of source apportionment calculations for particle number in the larger size bins because the tracer source mass in the larger size bin is no longer proportional to the number concentration from that source. This issue is relatively minor since size bins larger than 1µm that act as the dominant sink during particle coagulation events typically account for less than 5% of the total number concentration.

Perturbation studies were conducted to test the accuracy of the source apportionment calculations by setting the UFP emissions for on-road gasoline vehicles to zero during the month August 2012. Emissions of gases and emissions of larger particles from on-road vehicles were not changed. The difference between this perturbation simulation vs. the basecase simulation was calculated to estimate the number concentration of particles associated with on-road gasoline vehicles. This "zero-out" concentration was then compared to the standard model source-apportionment calculations in Figure 3 below. The two methods for number source apportionment yield very similar spatial patterns and very similar maximum concentrations of ~0.5 kcounts cm^{-3}. The tracer source apportionment method accounts for all particle sizes which produces slightly higher concentrations than the zero-out method that only considered particles smaller than 100 nm.

Formatted: Superscript

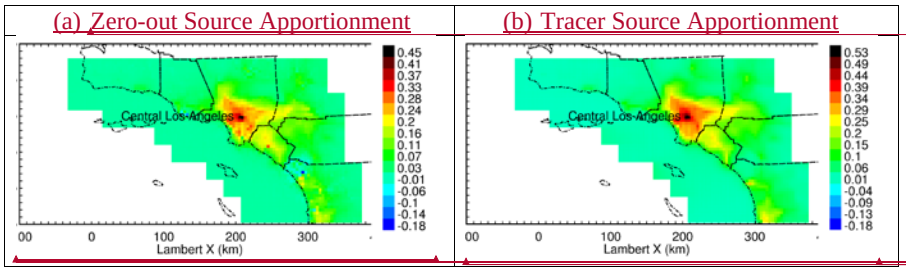

Figure 3: Particle number concentrations associated with on-road gasoline vehicles calculated using the zero-out method and the artificial tracer method in August 2012.

Many of the spatial patterns measured for airborne particle number concentrations in past studies have focused on the gradients around roads (see for example (Zhu et al., 2002a;Zhu et al., 2002b;Zhang et al., 2005;Zhang et al., 2004;Sowlat et al., 2016). These gradients are impossible to resolve using a regional model with 4km resolution. A limited set of additional simulations were conducted using the WRF/Chem model configured with Large Eddy Simulation (LES) around Oakland California so that spatial scales down to 250m could be examined. Maps of the predicted ultrafine particle mass concentrations for gasoline, diesel, food cooking, wood combustion, and natural gas combustion particles are shown in Figure 4 below. At 250m resolution, ultrafine particles from diesel engines peak on major transportation corridors while ultrafine particles from gasoline vehicles are more diffuse reflecting their increased activity on adjacent surface streets. Ultrafine particles from natural gas combustion are even more diffuse reflecting contributions from area sources across the region. As the spatial resolution decreases to 1km and then 4km, the fine details around roadways are artificially diluted in the larger grid cells. This process shifts the dominant source of ultrafine particles over roadways from diesel engines at 250m resolution to natural gas combustion at 4km resolution. These simulation results are consistent with measurements of particle number in the proximity of roadways which show that the traffic contribution to particle number concentration decays to background levels within 300 m (Zhu et al., 2002a;Zhu et al., 2002b). The measurements made by Zhu et al.

Formatted: Font color: Auto
Formatted: Line spacing: 1.5 lines
Formatted: Font: (Default) Times New Roman, 12 pt, Font color: Auto
Formatted: Font: (Default) Times New Roman, 12 pt, Font color: Auto
Formatted: Font: (Default) Times New Roman, 12 pt, Font color: Auto
Formatted: Font: (Default) Times New Roman, 12 pt, Font color: Auto
Formatted: Font: (Default) Times New Roman, 12 pt, Font color: Auto
Formatted: Font: (Default) Times New Roman, 12 pt, Font color: Auto

indicate that the traffic contribution to regional number concentration cannot be distinguished from other sources on a regional scale using 4km grid cells which is the focus of this study.

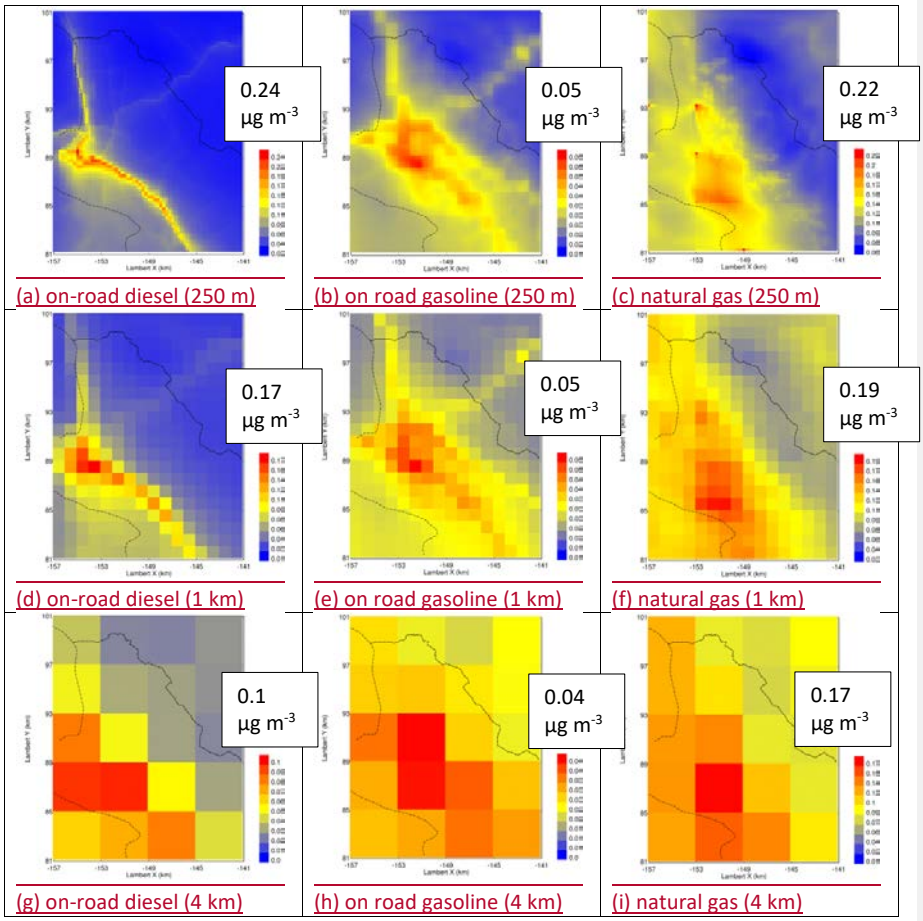

Figure 4: $PM_{0.1}$ mass concentration associated with on-road diesel, on-road gasoline, and natural gas combustion at 250m, 1km, and 4km resolution over Oakland, California.

Formatted: Line spacing: 1.5 lines

Formatted: Subscript

Formatted: Font: (Default) Times New Roman, 12 pt, Font color: Auto

405

~~The UCD/CIT model explicitly tracks the mass and the number concentration of particles in each size bin, with tracer species used to quantify source contributions to the primary particle mass (but not number) in that bin. Tracer emissions are empirically set to be 1 % of the total primary particle mass emitted from each source category. This minor~~

410 ~~addition does not significantly change the particle radius. Tracers are carried through all major aerosol processes including advection, diffusion, coagulation, and deposition. The~~

~~final tracer concentrations are therefore directly proportional to the primary particle mass from the associated source group. More details describing the source apportionment technique in UCD/CIT model are provided in the previous studies (Ying et al., 2008b;Hu et al., 2017). In the current study, the mass contribution from each source was converted to the number contribution from that source according to equation 1:~~

~~$number_i = mass_i / (\pi/6 * Dp^3 * \rho)$ (1)~~

~~where $number_i$ is the number concentration associated with source *i*, $mass_i$ is the mass concentrations associated with source *i*, Dp is the particle diameter and ρ is the particle density (calculated based on particle composition). This approach assumes that the condensation of new mass does not strongly affect the calculated density of the particles (true when condensation is not dominant in the size bins that contain most of the particle number). The accuracy of this assumption was tested by comparing the sum of the "reconstructed" particle number (eq 1) across all sources to the actual total particle number tracked by the model yielding error <10% in the current study.~~

3.2.1 UCD/CIT $PM_{0.1}$ source contributions compared to Chemical Mass Balance (CMB) results

A recently completed study measured the composition of $PM_{0.1}$ at four sites in California and calculated source contributions using molecular markers (Xue et al., 2018b). Figures 5~~2~~ and 6~~3~~ compare the source contributions to PM0.1 OC concentrations predicted by the UCD/CIT model and "measured" using the molecular marker technique at San Pablo, East Oakland, downtown Los Angeles and Fresno during a summer month (August 2015) and a winter month (February 2016). The "others" category in the molecular marker calculation represents unresolved sources, while in the UCD/CIT model "others" represents the sum of non-residential natural gas source combustion, aircraft emissions, and the sources that were not tagged in the current study. In general, the ranking and concentration range of ~~predicted~~ source contributions to PM0.1 OC from the molecular marker technique and the UCD/CIT model are consistent~~are in good agreement~~. Natural

gas dominates PM0.1 OC in the summer of 2015 at San Pablo, East Oakland, downtown Los Angeles and Fresno, while wood smoke and aircraft are the major sources of PM0.1 OC in Fresno and East Oakland during the winter of 2016. The importance of ultrafine particles from natural gas combustion has not previously been recognized because these particles lack a unique chemical signature, which causes them to be lumped into the "unresolved" category in receptor-based source apportionment studies. The ~~general agreement in the~~ source contribution results ~~from~~ for the gasoline, diesel, wood burning, meat cooking and other source categories predicted by the UCD/CIT model and the molecular marker technique illustrated in Figures 5 and 6 build~~s~~ confidence in the accuracy of the UFP source predictions in the current study.

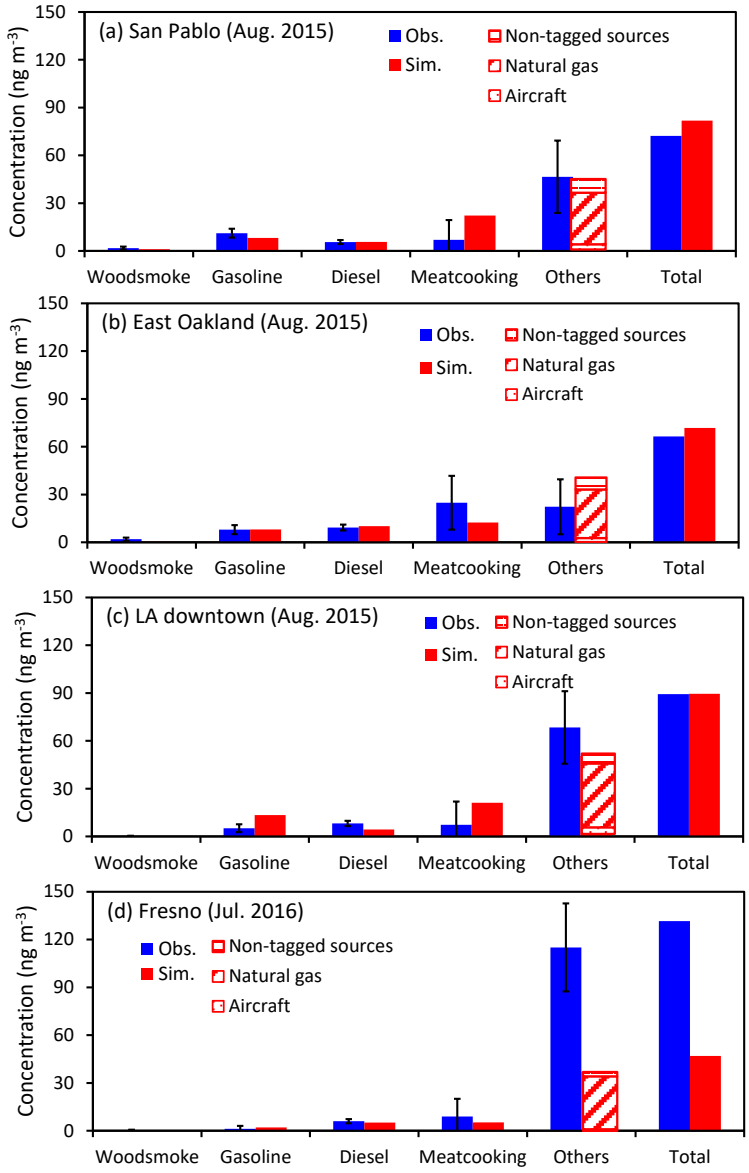

Figure 5~~2~~: Source contribution to PM0.1 predicted by the CMB receptor model and the UCD/CIT model at four sites in California in August 2015. CMB results are calculated using 3-day average measurements composited for a full month.

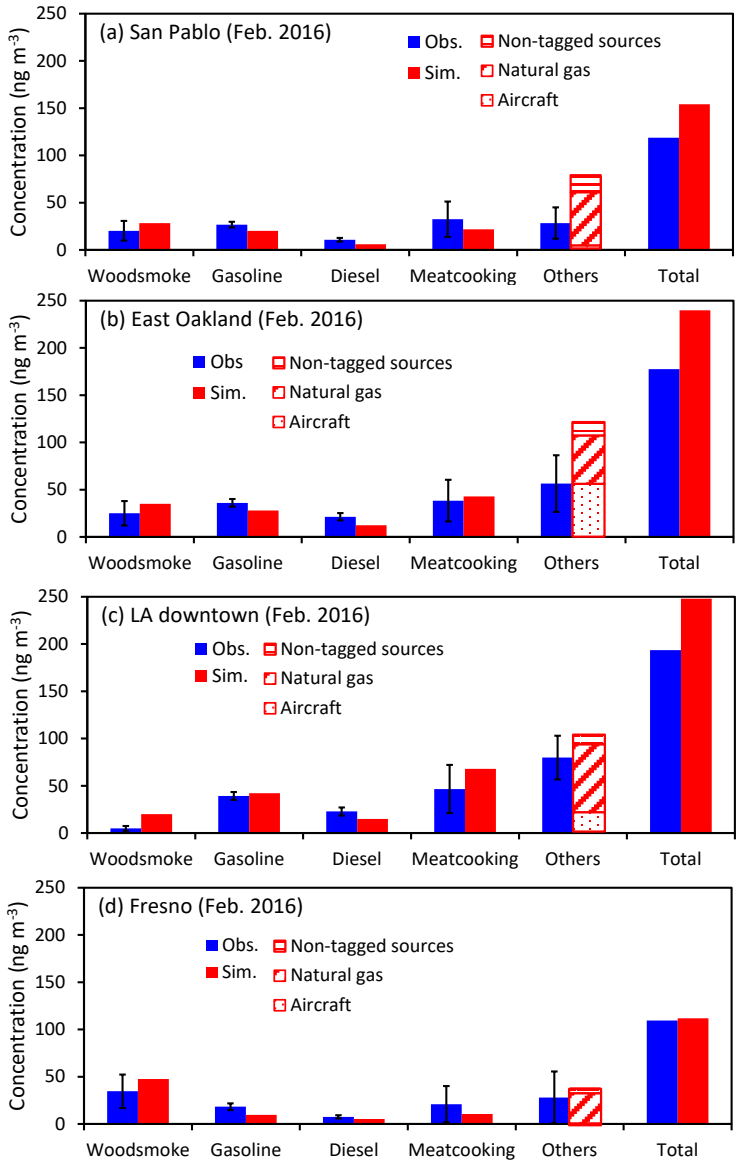

Figure 6~~3~~: Source contribution to PM0.1 predicted by the CMB receptor model and the UCD/CIT model at four sites in California in February 2016. CMB results are calculated using 3-day average measurements composited for a full month.

3.2.2 $PM_{0.1}$ and $N_{10\text{-}1000}$ Source contributions in California

Figures 7-94-6 and 10-127-9 show the seasonal variation of major source contributions to primary PNCN_{10} and $PM_{0.1}$, respectively. The black circles in Figure 7-94-6 represent the measured $N_{7\text{-}1000}$ at four BAAQMD sites in SFBA and six MATES sites in Los Angeles and Riverside counties. Predicted "best-fit" PNC N_{10} follows the same trends as agrees reasonably well with mmeasured seasonal variations of $N_{7\text{-}1000}$ at Livermore, San Pablo, Redwood City, LivermoreSanta Rosa, Anaheim, Central LA, Compton and Huntington Park, Inland Valley, and Rubidoux. The model under predicts $N_{7\text{-}1000}$ at Santa Rosa and over predicts $N_{7\text{-}1000}$ at Anaheim, central Los Angeles, and ComptonInland Valley and Rubidoux but overall model performance statistics for N_7 PNC are within the target range guidelines for regulatoryfor $PM_{2.5}$ applications (see Table 1). Nucleation contributes to summer PNCN_{10} at all sites but makes negligible contributions to $PM_{0.1}$ concentrations. Traffic sources including gasoline- and diesel-powered vehicles make significant contributions to $PM_{0.1}$ concentrations at each measurement site depending on proximity to major freeways. Near-roadway effects on ultrafine particle concentrations are not apparent since these locations were chosen to be regional monitors and so they are more than 300 m from the nearest freeway. Predicted contributions from traffic sources are consistent with the molecular marker results illustrated in Figures 5-62-3. Traffic contributions to regional PNC N_{10} concentrations more than 300 m away from roadways are even smaller than $PM_{0.1}$ contributions because the size distribution of particles emitted from motor vehicles peaks at 100 – 200 nm (Robert et al., 2007a;Robert et al., 2007b). Wood smoke makes strong contributions to regional $PM_{0.1}$ concentrations in central California during winter but much smaller contributions in the SoCAB because wood burning is not typically used for home heating in this region. Wood burning contributions PNC N_{10} are less dominant in central California because the size distribution of particles emitted from wood combustion peaks at 100-300 nm (Kleeman et al., 2008a). The largest primary source of PNC N_{10} in central California and PNCN_{10}+$PM_{0.1}$ in the SoCAB is non-residential natural gas combustion. Industrial processes and power generation that use natural gas do not follow strong seasonal cycles

and so the strength of the natural gas source contributions is somewhat constant across seasons subject to variability caused by meteorological conditions.

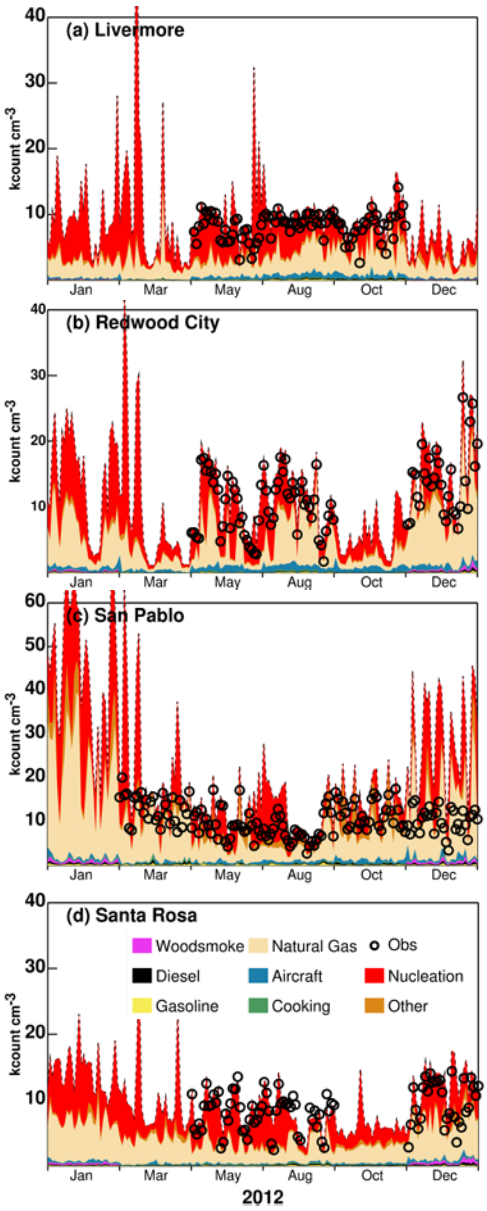

Figure 74: Seasonal variation of measured N_{7-1000} (black circles) and major source contributions to "best-fit" ~~PNC~~ N_{10} at Livermore, Redwood City, San Pablo and Santa Rosa, respectively. Results within each month have daily time resolution.

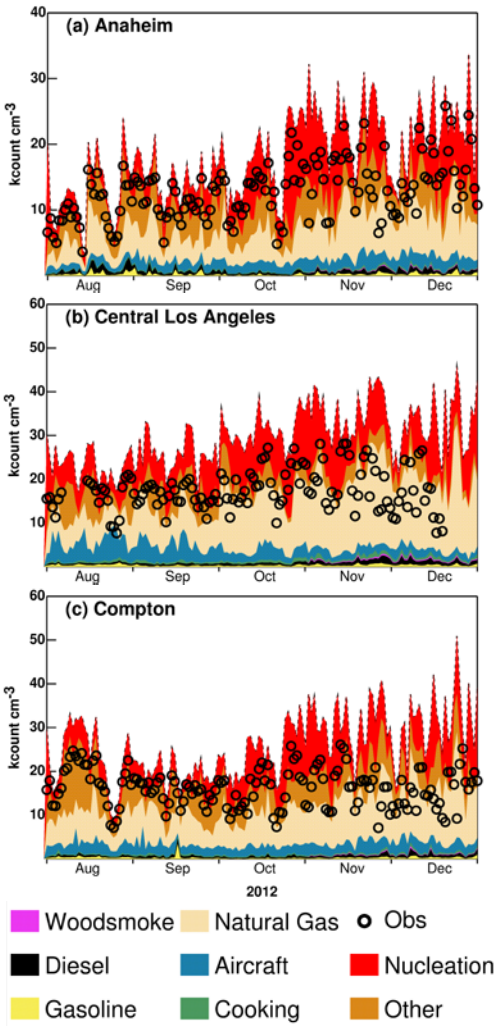

Figure 85: Seasonal variation of measured N_{7-1000} (black circles) and major source contributions to "best-fit" PNC N_{10} at Anaheim, Central LA, and Compton, respectively. Results within each month have daily time resolution.

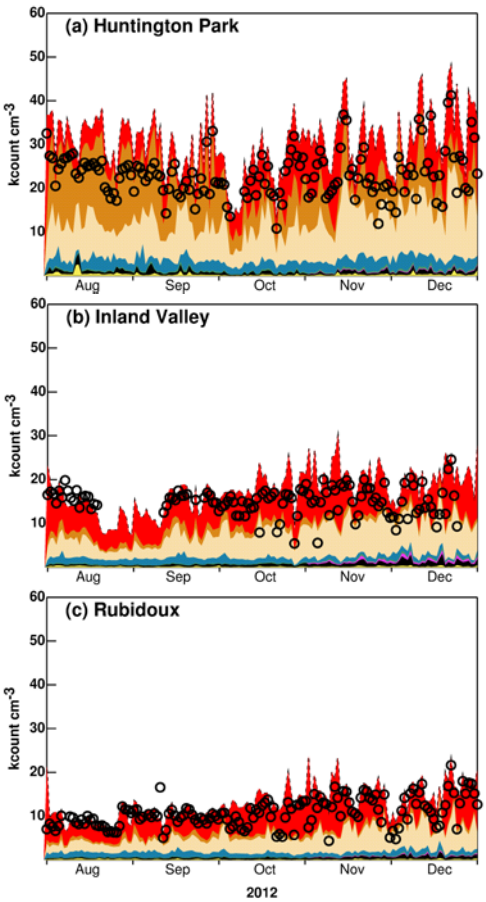

Figure 9~~6~~: Seasonal variation of measured N_{7-1000} (black circles) and major source contributions to "best-fit" ~~PNC~~ N_{10} at Huntington, Inland-Valley, and Rubidoux, respectively. Results within each month have daily time resolution.

505

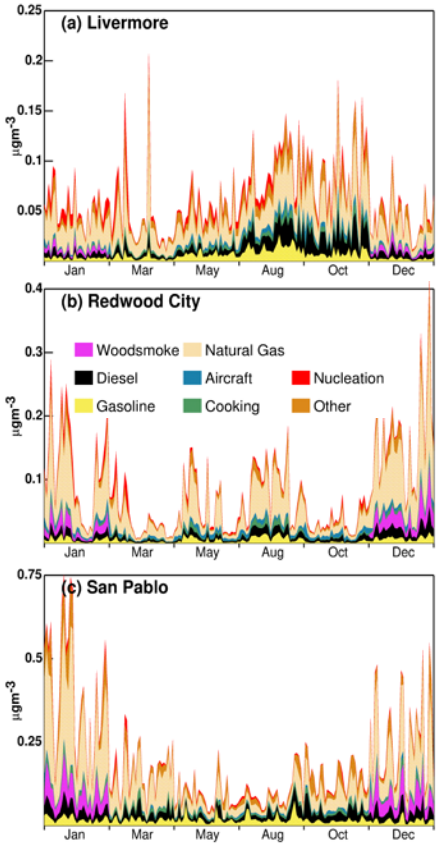

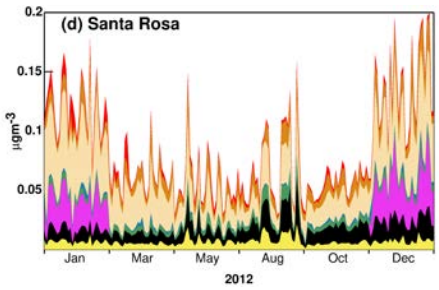

Figure 10~~7~~: Seasonal variation of major source contributions to $PM_{0.1}$ at Livermore, Redwood City, San Pablo and Santa Rosa, respectively. Results within each month have daily time resolution.

510

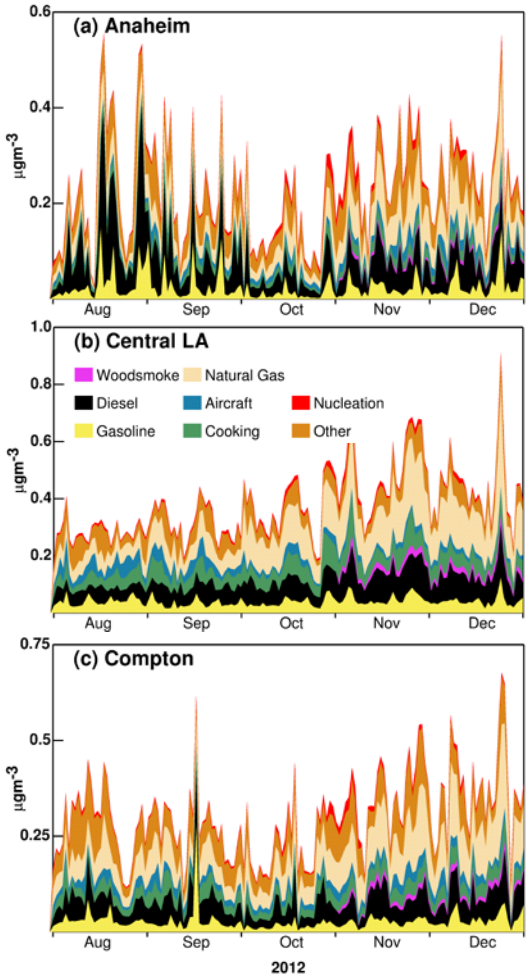

Figure 11~~8~~: Seasonal variation of major source contributions to $PM_{0.1}$ at Anaheim, Central LA, and Compton, respectively. Results within each month have daily time resolution.

515

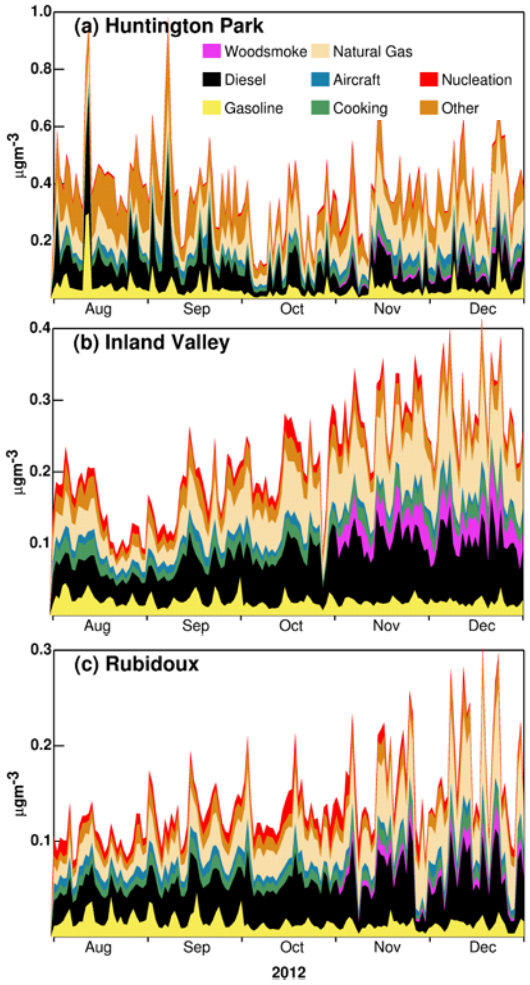

Figure 12~~9~~: Seasonal variation of major source contributions to PM0.1 at Huntington, Inland-Valley, and Rubidoux, respectively. Results within each month have daily time resolution.

520

Figures 13~~10~~ and Figures 14~~11~~ show the source contributions to ~~PNC~~ N_{10} and $PM_{0.1}$, respectively, averaged over the days shown in Figures 7-9~~4-9~~. Aside from nucleation, n~~N~~on-residential natural gas combustion makes the largest predicted primary contribution to ~~PNC~~ N_{10} at all the sites that were evaluated. Traditional sources that were tracked including meat cooking, wood smoke, and mobile (gasoline + diesel) accounted for approximately 5-15~~10-20~~% of the predicted ~~PNC~~ N_{10} at the sites selected for study. "Other" sources that were not tagged explicitly in the current study accounted for 5-31~~8-28~~% of ~~PNC~~ N_{10} across these sites. Nucleation is a significant source for of ~~PNC~~ N_{10} for both BAAQMD sites and MATES sites where sulfur emissions were highest, with contributions ranging from 24-57~~6-14~~%.

The ~~dominant~~ strong ~~PNC~~ N_{10} contribution from ~~non-residential~~ natural gas combustion reflects the emitted particle size distribution combined with the ubiquitous use of this fuel in the SFBA and SoCAB regions. The chemical composition and size distribution information for non-residential natural gas combustion emissions used in this study was measured by Hildemann (1991) and Li and Hopke (1993), respectively. Size distributions and volatility were further confirmed during on-going field studies conducted by the current authors (Xue et al., 2018a). The estimated non-residential natural gas combustion particle number and mass size distributions are shown in Figure S1 (left column). Clearly, the majority of particles from non-residential natural gas combustion are typically found in diameters <0.05 µm, while particles emitted from other sources such as wood combustion tend to have slightly larger particle diameter (with lower number concentration per unit of emitted mass). These natural gas particles grow through the condensation of SOA once in the atmosphere, but they still contribute strongly to N_{10} concentrations.

Figure~~s~~ 1~~4~~1 show~~s~~ that on-road vehicles (gasoline and diesel combined) are ~~wood smoke is~~ the largest $PM_{0.1}$ source at Anaheim ~~Livermore~~ (3~~9~~6%), central LA~~San Pablo~~ (3~~1~~5%), Huntington Park (33%), Inland Valley (39%), and Rubidoux (42%), while ~~non-residential~~ natural gas combustion still makes the largest contribution to $PM_{0.1}$ at other evaluation sites~~Redwood City (28%), Santa Rosa (41%) and MATES sites (42%-58%) in the SoCAB region~~. Contributions from cooking and mobile sources are enhanced in $PM_{0.1}$ vs.

~~PNC~~N_{10}, with the cooking source accounting for 1~~5~~% of $PM_{0.1}$ at Santa Rosa. ~~and mobile sources (gasoline + diesel) accounting for 34% of $PM_{0.1}$ at the Central LA site, followed by 33% of $PM_{0.1}$ at Livermore site.~~ The different rankings of source contributions to ~~PNC~~ N_{10} and $PM_{0.1}$ can be explained by the comparison of particle number-size distribution and particle mass-size distribution for the non-residential natural gas and wood burning sources at four evaluated sites (Figure S1). Particles emitted from non-residential natural gas combustion and wood burning have number distributions that peak at particle diameters of 0.016-0.025 µm and 0.025-0.04 µm, respectively. Non-residential natural gas combustion and wood burning mass distributions, however, peak at particle diameters of 0.025-0.04 µm and 0.10-0.16 µm, respectively.

Figure 15-17~~12-14~~ show diurnal variations of measured $N_{7\text{-}1000}$ and predicted "best-fit" ~~PNC~~ N_{10} averaged over days in August and December 2012. Measured $N_{7\text{-}1000}$ diurnal patterns in August generally peak in the afternoon hours between 12-3pm with an optional morning peak around 6am~~are bimodal with the first peak usually occurring at 6-7 am at four sites in SFBA and 5-6 am at six sites in Los Angeles and Riverside County and the second peak occurring between 12-3 pm~~. The ~~first summer peak corresponds to morning activities including cooking and traffic "rush hours", while the~~ main ~~second~~afternoon peak appears to be related to nucleation events while the smaller early-morning peak appears to be related to early morning human activity including natural gas combustion. The predicted "best-fit" ~~PNC~~ N_{10} diurnal variations in August followed the same trends as ~~were in good agreement with~~ measurements at ~~five~~ six out of ten sites (Livermore, Anaheim, Compton, Huntington Park, Inland Valley, and Rubidoux). ~~San Pablo, Anaheim, Compton, and Huntington). The model generally predicts a biomodal diurnal profile with maximum values in reasonable agreement with measurements at these locations.~~ The model failed to capture the mid-day nucleation event at Redwood City and Santa Rosa possibly due to missing SO_2 sources in the emissions inventory upwind from these~~is~~ sites. The model overestimated mid-day peak values at Anaheim and central Los Angeles~~Inland valley and Rubidoux sites~~. In December, the measured $N_{7\text{-}1000}$ diurnal pattern were~~as also~~ more distinctly bimodal with the first peak around 7:00-8:00am and the second peak in the evening at around 8pm. This pattern reflects both the emissions activity and the mixing status of the atmosphere throughout the day. The

predicted "best-fit" ~~PNC~~ N_{10} concentration follows this same pattern. ~~is in good agreement with measurements for the early morning peak but generally underestimated the evening peak possibly due to excess atmospheric mixing after sunset in the model calculations.~~ Nucleation continues to ~~appears to~~ play a ~~small~~ role during winter but does not dominate to the point that it produces a midday peak in N_{10} concentrations . Non-residential natural gas combustion is predicted to be the largest source of ~~PNC~~ N_{10} during morning and evening peaks. The diurnal profiles of non-residential natural gas emissions are included in supplemental information (Figure S2) along with the regional distribution of those emissions (Figure S3). These diurnal variation of the natural gas combustion emissions were obtained directly from the emissions inventory specified by the California Air Resources Board. Industrial natural gas combustion emissions peak during the daytime with lower values at night. Emissions from electricity generation powered by natural gas peak in the morning and evening. Commercial natural gas combustion emissions may either peak in the morning and evening or they may follow a uniform diurnal profile depending on the specific source and location.

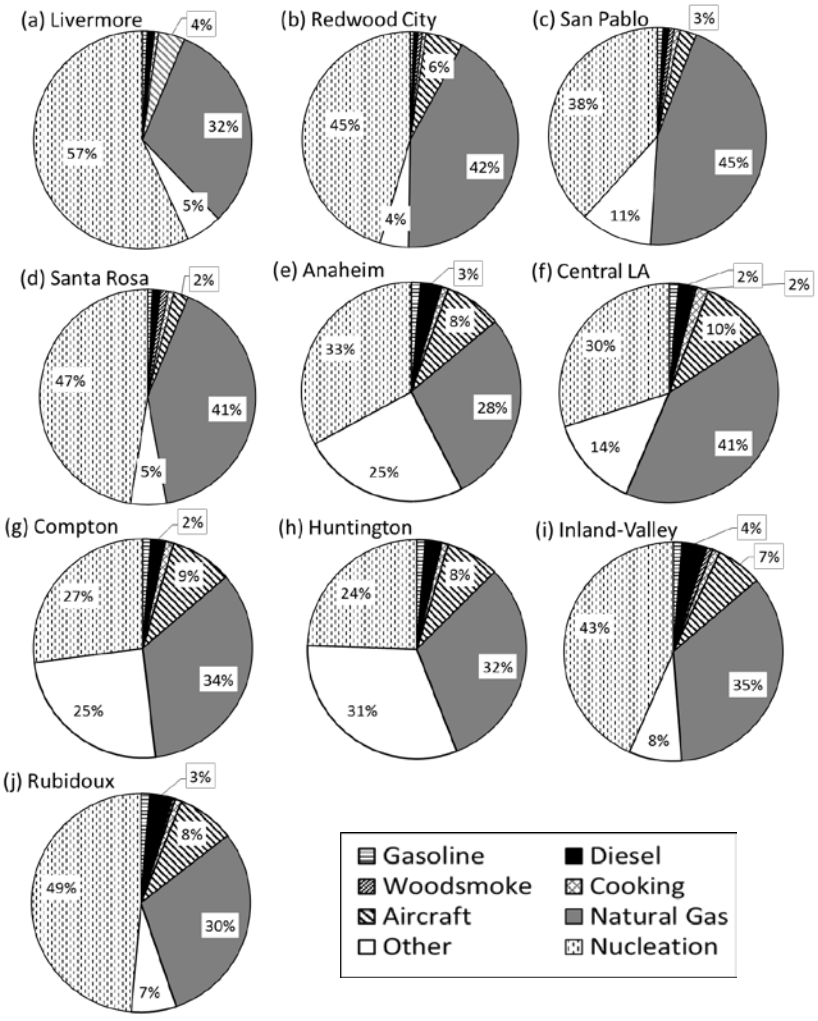

Figure 1~~3~~0: The relative source contributions to ~~PNC~~ N_{10} at Livermore, Redwood City, San Pablo, Santa Rosa, Anaheim, Central LA, Compton, Huntington, Inland-Valley and Rubidoux, respectively. Averaging time included all days shown in Figures 7-9~~4-6~~. Values not displayed are ≤ 1%.

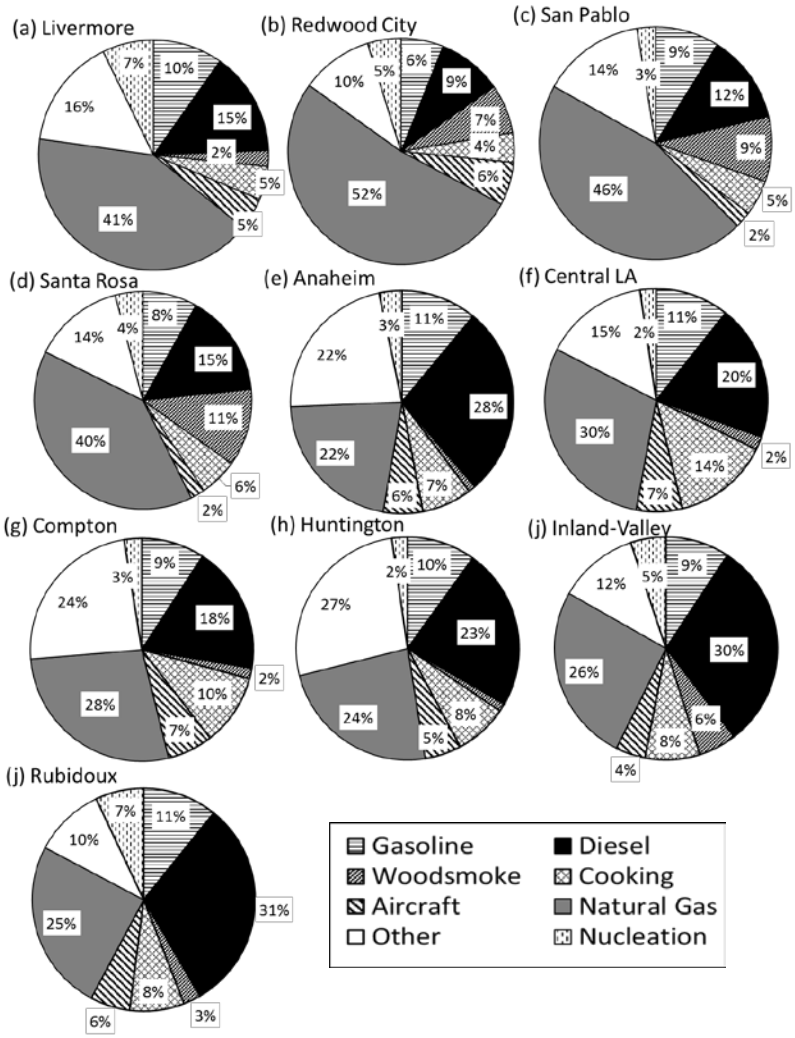

Figure 1~~1~~: The relative source contributions to $PM_{0.1}$ seasonally averaged at Livermore, Redwood City, San Pablo and Santa Rosa, Anaheim, Central LA, Compton, Huntington, Inland-Valley and Rubidoux, respectively. Averaging time included all days shown in Figures 10-12~~7-9~~. Values not displayed are ≤ 1%.

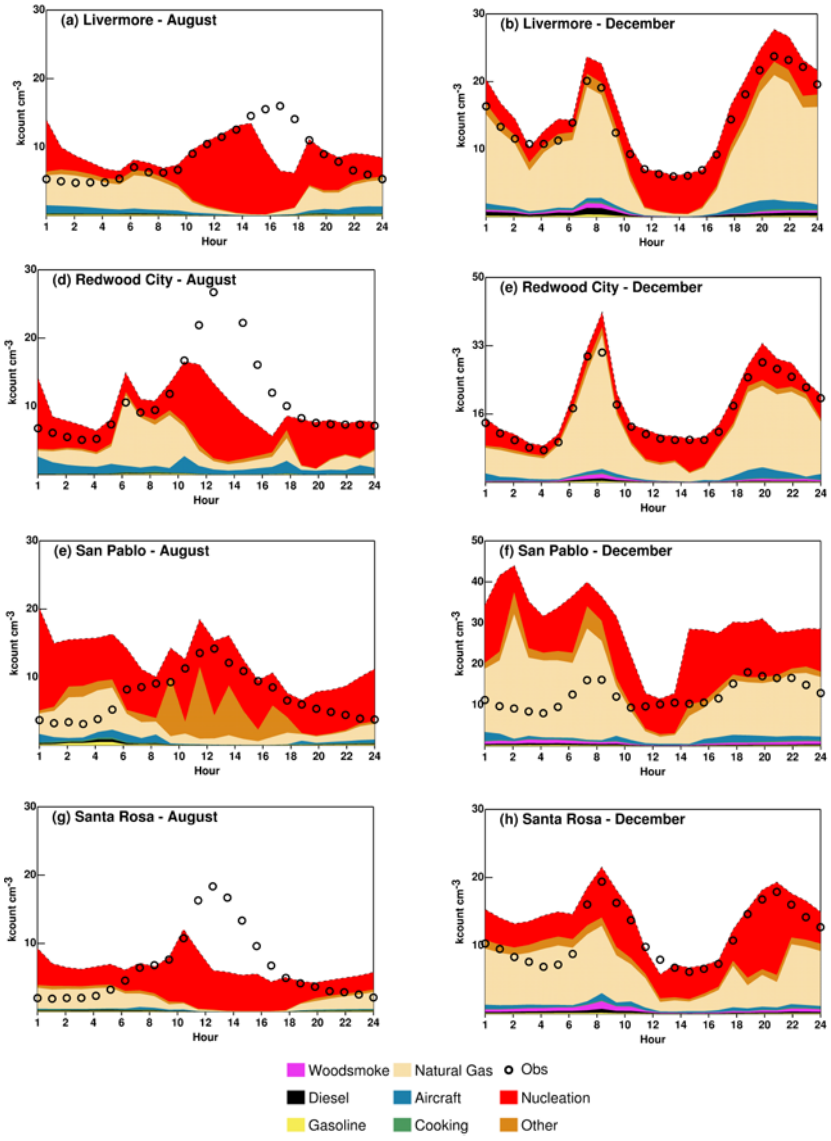

Figure 1~~5~~2: Diurnal variations of measured N_{7-1000} and predicted "best-fit" ~~PNC~~ N_{10} averaged for August 2012 (left column) and December 2012 (right column) at Livermore, Redwood City, San Pablo and Santa Rosa.

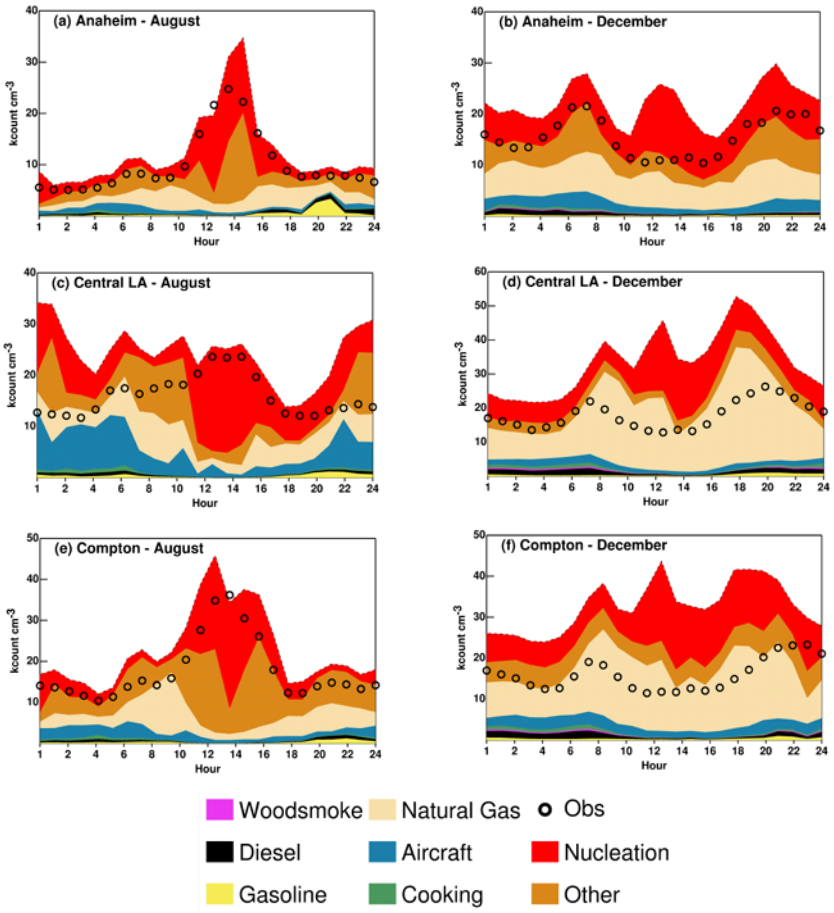

Figure 1~~6~~3: Diurnal variations of measured N_{7-1000} and predicted "best-fit" ~~PNC~~ N_{10} averaged for August 2012 (left column) and December 2012 (right column) at Anaheim, Central LA, and Compton.

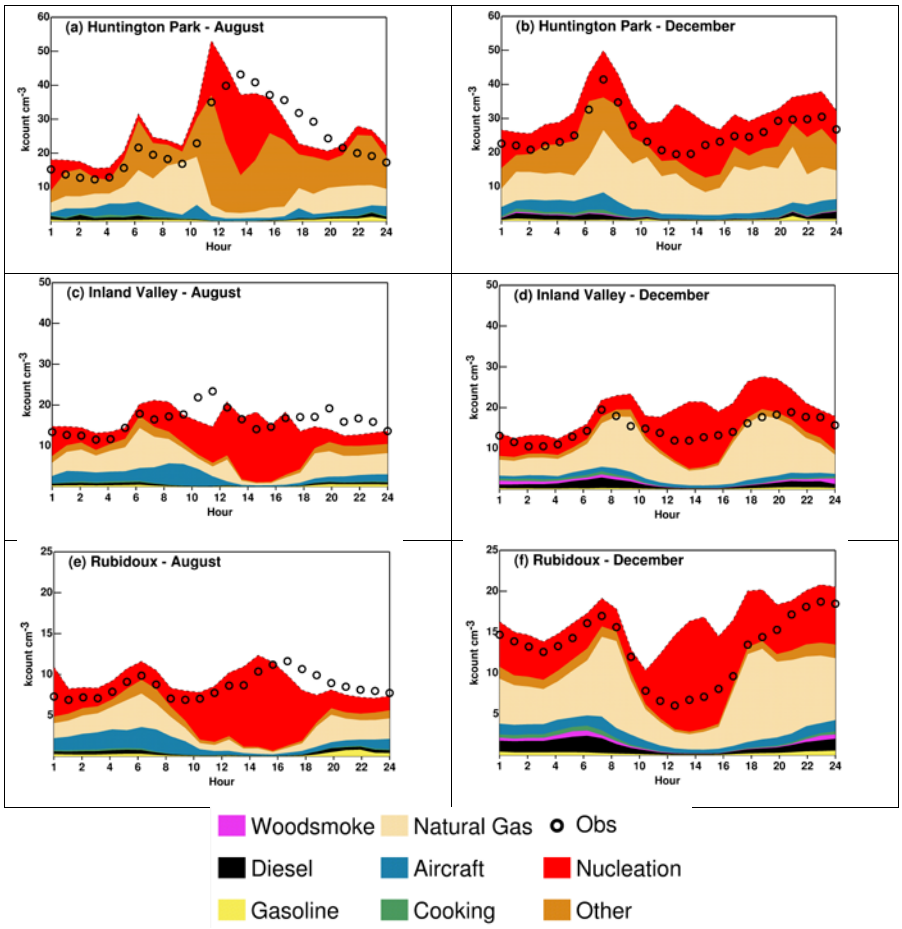

Figure 1~~7~~4: Diurnal variations of measured N_{7-1000} and predicted "best-fit" ~~PNC~~ N_{10} averaged for August 2012 (left column) and December 2012 (right column) at Anaheim, Central LA, and Compton.

3.2.3 Regional $N_{10-1000}$ Source contributions in California

Figure 18 illustrates the predicted number concentration associated with primary emissions (Figures 18a-i) and nucleation (Figure 18j) in southern California averaged

over the months Aug-Dec 2012. Figure 18g shows that primary aircraft emissions in the plume downwind of the Los Angeles International Airport (LAX) are predicted to account for 8 kcounts cm^{-3} and Figure 18j shows that nucleation of aircraft emissions in the LAX plume are predicted to account for 45 kcounts cm^{-3} yielding a total number concentration associated with LAX aircraft of approximately ~53 kcounts cm^{-3}. Hudda et al. (2014) found that particle number concentrations increased by a factor of four to eight downwind of LAX based on measurements in June-July 2013. Total ground-level number concentrations in the LAX plume reached 60-70 kcounts cm^{-3}. Given the 4km spatial resolution of the model calculations used in the current study, the predictions and measurements of particle number concentration downwind of LAX are consistent with one another.

Formatted: Superscript

Formatted: Superscript

Formatted: Superscript

Formatted: Superscript

It is noteworthy that military airbases in Figure 18g have significantly higher particle number concentrations due to their use of aviation fuel with higher sulfur content, but nucleation plumes are not present downwind of these locations (Figure 18j). Particles emitted from military aircraft are represented as primary emissions in the current model calculations. Future measurements should compare particle number concentrations downwind of civilian and military airports to fully evaluate the impact of aviation fuel sulfur content on ambient ultrafine particle concentrations.

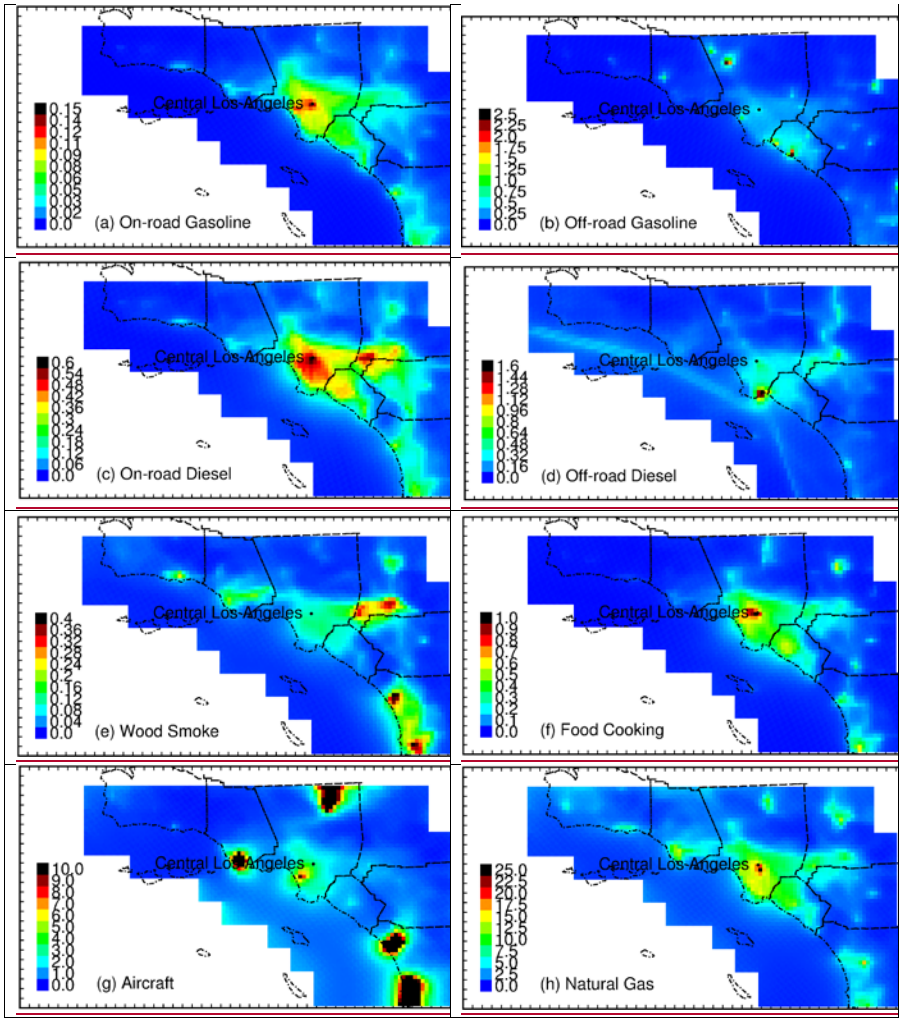
Central Los Angeles
0.15
0.14
0.12
0.11
0.09
0.08
0.06
0.05
0.03
0.02
0.0
(a) On-road Gasoline
Central Los Angeles
2.5
2.25
2.0
1.75
1.5
1.25
1.0
0.75
0.5
0.25
0.0
(b) Off-road Gasoline
Central Los Angeles
0.6
0.54
0.48
0.42
0.36
0.3
0.24
0.18
0.12
0.06
0.0
(c) On-road Diesel
Central Los Angeles
1.6
1.44
1.28
1.12
0.96
0.8
0.64
0.48
0.32
0.16
0.0
(d) Off-road Diesel
Central Los Angeles
0.4
0.36
0.32
0.28
0.24
0.2
0.16
0.12
0.08
0.04
0.0
(e) Wood Smoke
Central Los Angeles
1.0
0.9
0.8
0.7
0.6
0.5
0.4
0.3
0.2
0.1
0.0
(f) Food Cooking
Central Los Angeles
10.0
9.0
8.0
7.0
6.0
5.0
4.0
3.0
2.0
1.0
0.0
(g) Aircraft
Central Los Angeles
25.0
22.5
20.0
17.5
15.0
12.5
10.0
7.5
5.0
2.5
0.0
(h) Natural Gas

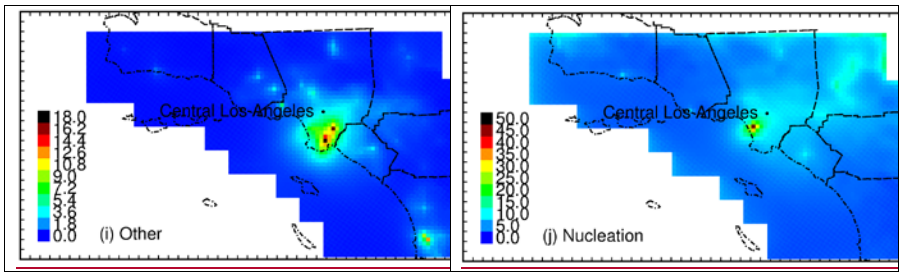

Figure 18. Spatial distribution of particle number from major sources in Southern California (unit: kcount cm^{-3}).

Figure 19 illustrates the predicted particle number concentrations associated with primary sources and nucleation in northern California. The relative importance of sources and the prediction of nucleation downwind of major sulfur emissions are consistent in northern and southern California. Natural gas combustion is a notable strong source of ultrafine particles in both regions due to the widespread use of this fuel in numerous residential, commercial, and industrial applications. In many cases, the natural gas combustion particles contribute strongly to the "urban background' concentrations over most California cities without the formation of individual plumes such as those found downwind of LAX. Future measurements could correlate ambient particle number concentrations and natural gas utilization across multiple cities to evaluate whether natural gas combustion is a significant source of particle number concentration.

Formatted: Superscript

Formatted: Font: (Default) Times New Roman, 12 pt

Formatted: Font: (Default) Times New Roman, 12 pt

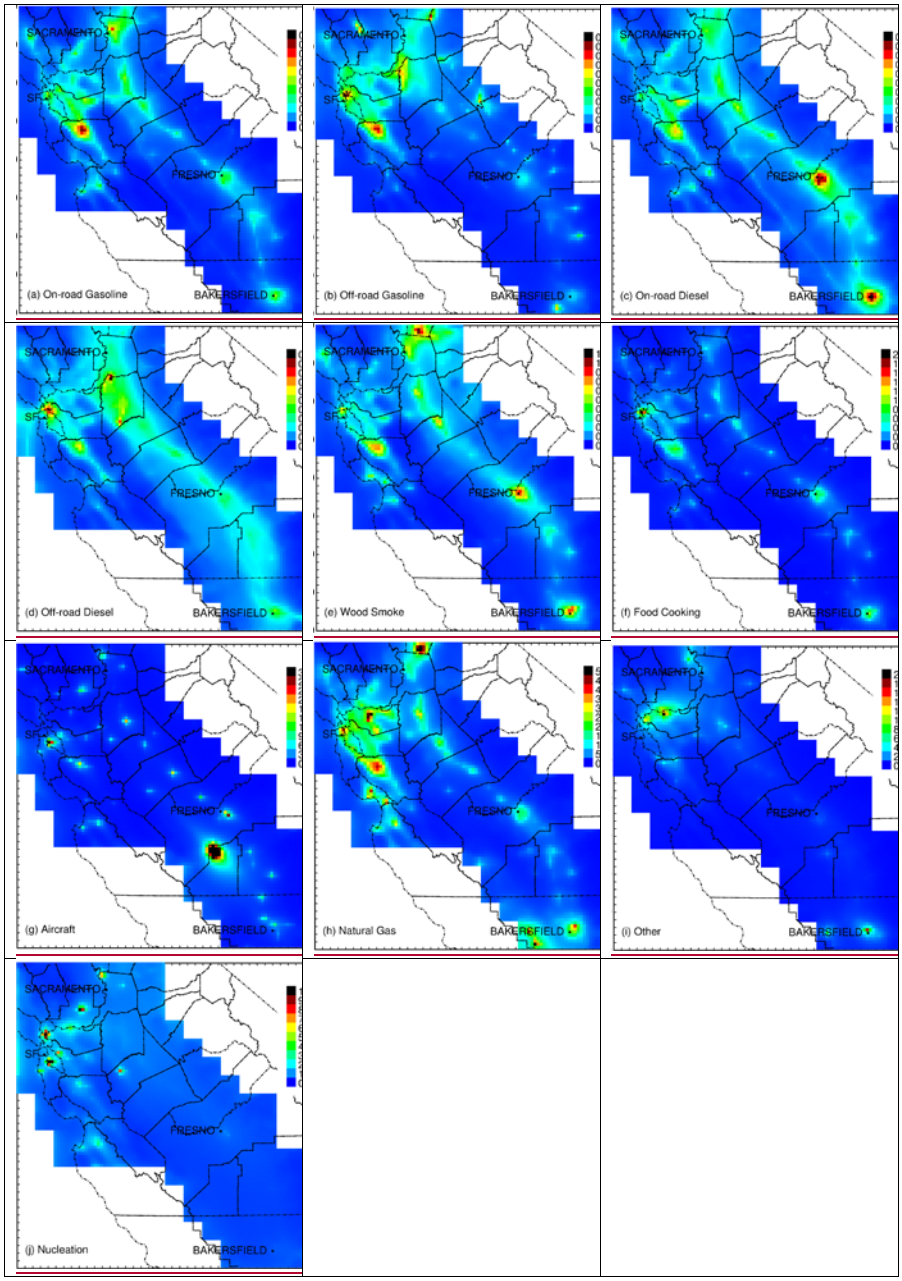
SACRAMENTO
SF
FRESNO
BAKERSFIELD
(a) On-road Gasoline
(b) Off-road Gasoline
(c) On-road Diesel
(d) Off-road Diesel
(e) Wood Smoke
(f) Food Cooking
(g) Aircraft
(h) Natural Gas
(i) Other
(j) Nucleation

Figure 19. Spatial distribution of particle number from major sources in Northern California (unit: kcount cm^{-3}).

The concentrations of nucleated particles in August, October, and December are shown in Figure 20 (Southern California) and Figure 21 (Northern California) below. Nucleation events occur in the regions where sulfur emissions are highest (typically airports, shipping ports and refining facilities). Concentrations of nucleated particles are higher in October and December than in August because colder temperatures increase nucleation rates if the precursor H_2SO_4 and NH_3 concentrations are relatively constant. A significant fraction of the H_2SO_4 in the current simulation is produced by the fast conversion of gas-phase SO_3 emissions to H_2SO_4 in the exhaust plume near the emissions source. SO_3 conversion does not depend on the presence of oxidants in the atmosphere and so the higher oxidant concentrations in the summer do not dominate the seasonal nucleation pattern.

Once H_2SO_4 forms in the exhaust plumes, it either condenses onto existing particles formed from lower volatility compounds in the plume, or it mixes with NH_3 in the background air and nucleates. This process is captured by dilution source sampling measurements that allow for a few minutes of aging time and so the size-resolved emissions profiles for many sources already account for the effects of nucleation within the "near-field" exhaust plume (within a few 10's of meters after emission). SO_3 emissions from reciprocating internal combustion engines were therefore set to zero to avoid double counting the new particle formation downwind of these sources in the current study. Regular SO_2 emissions from these sources were not modified. Emissions from aircraft jet engines have high exit velocity which promotes rapid mixing with background air. SO_3 emissions were left at their nominal levels (3-4% of total SOx) for jet engine aircraft in the current study. The consequence of these model treatments is that predicted concentrations of nucleated particles are highest downwind of LAX, which agrees with measurements of ambient particle number concentrations (Hudda et al., 2014).

Formatted: Superscript

Formatted: Font: (Default) Times New Roman, 12 pt

Formatted: Font: 12 pt

Formatted: Font: 12 pt

Formatted: Font: 12 pt

Formatted: Font: 12 pt, Subscript

Formatted: Font: 12 pt

Formatted: Font: 12 pt, Subscript

Formatted: Font: 12 pt

Formatted: Font: 12 pt, Subscript

Formatted: Font: 12 pt

Formatted: Font: 12 pt, Subscript

Formatted: Font: 12 pt

Formatted: Font: 12 pt, Subscript

Formatted: Font: 12 pt

Formatted: Font: 12 pt, Subscript

Formatted: Font: 12 pt

Formatted: Font: 12 pt, Subscript

Formatted: Font: 12 pt

Formatted: Font: 12 pt, Subscript

Formatted: Font: 12 pt

Formatted: Font: 12 pt, Subscript

Formatted: Font: 12 pt

Formatted: Font: 12 pt

Formatted: Font: 12 pt, Subscript

Formatted: Font: 12 pt

Formatted: Font: 12 pt, Subscript

Formatted: Font: 12 pt

Formatted: Font: 12 pt, Subscript

Formatted: Font: 12 pt

Formatted: Font: 12 pt, Subscript

Formatted: Font: 12 pt

Formatted: Font: 12 pt, Subscript

Formatted: Font: 12 pt

Formatted: Font: 12 pt

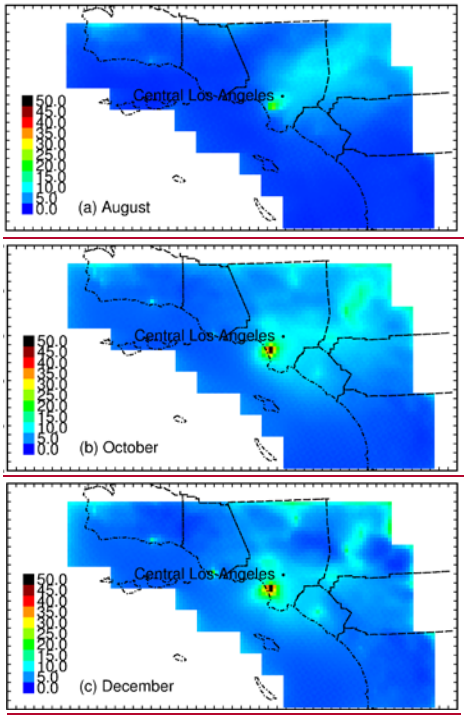

Figure 20: Seasonal variation of nucleated particle concentrations in Southern California. Units are kcount cm^{-3}.

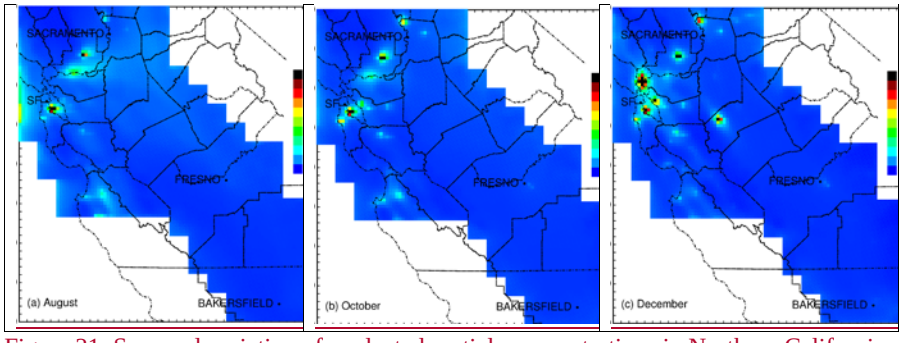

Figure 21: Seasonal variation of nucleated particle concentrations in Northern California. Units are kcount cm^{-3}.

Formatted Table

Formatted: Font: (Default) Times New Roman, 12 pt

Formatted: Font: (Default) Times New Roman, 12 pt

Formatted: Font: (Default) Times New Roman, 12 pt

Formatted: Superscript

Formatted: Font: (Default) Times New Roman, 12 pt

Formatted: Font: (Default) Times New Roman, 12 pt

Formatted: Font: (Default) Times New Roman, 12 pt

Formatted: Font: (Default) Times New Roman, 12 pt

Formatted: Font: (Default) Times New Roman, 12 pt

Formatted: Font: (Default) Times New Roman, 12 pt

Formatted: Font: (Default) Times New Roman, 12 pt

Formatted: Font: (Default) Times New Roman

Formatted: Line spacing: 1.5 lines

4. Discussion

Previous researchers have used Positive Matrix Factorization (PMF) to calculate source contributions to ~~PNC~~ N_7 (Sowlat et al., 2016;Morawska et al., 2008;Gu et al., 2011;Ogulei et al., 2007;Kasumba et al., 2009;Wang et al., 2013;Yue et al., 2008;Friend et al., 2013). The dominant factors resolved by these studies have been traffic, urban background, secondary aerosol, wood burning and nucleation (Sowlat et al., 2016;Morawska et al., 2008;Gu et al., 2011;Ogulei et al., 2007;Kasumba et al., 2009;Wang et al., 2013;Yue et al., 2008;Friend et al., 2013). Particles from natural gas combustion were not separately identified by PMF because they do not contain a unique chemical tracer. It is very likely that natural gas combustion particles are artificially lumped into another source (e.g. traffic) or part of the "urban background" signal identified in previous studies. Natural gas combustion is used extensively in California for electric power, industrial, commercial and residential use (Table S6), and so it seems plausible that this source contributes to ambient UFP concentrations.

The current UFP predictions rely on source profile measurements for wood burning, food cooking, mobile sources, and non-residential natural gas combustion (Cooper, 1989;Harley et al., 1992;Hildemann et al., 1991a;Hildemann et al., 1991b;Houck and L. C., 1989;Kleeman et al., 2008b;Kleeman et al., 2000;Robert et al., 2007b;Robert et al., 2007a;Schauer et al., 1999b, a, 2001, 2002b, a;Taback, 1979). All of these size distributions were measured using appropriate instruments and methods by knowledgeable researchers, but some of these past studies were conducted more than a decade ago. Size distribution information for vehicles, natural gas, etc. have been added to the supplemental information (Figure S4~~3~~). Changes in fuel composition and emissions control technology in the interim years may have altered the emitted size distributions. New measurements of particle size distributions emitted from natural gas and biomethane combustion were made in parallel with the current project to confirm the source profile measurements from past studies (Xue et al., 2018a). The results of these measurements are consistent with previous size distribution results.

California has tighter air pollution standards than many other regions in the United States due to the severe air quality problems that have historically occurred in the state.

California therefore has a unique ~~mixture~~ combination of fuels and emissions control technology that may affect the mixture of sources that contribute to atmospheric ultrafine particle concentrations. Venecek et al. (2018) recently used the UCD/CIT air quality model with the 2011 National Emissions inventory to calculate source contributions to $PM_{0.1}$ in 39 major cities across the United States during peak summer photochemical smog episodes in the year 2010. The findings from this study show that natural gas combustion is a major source of ultrafine particles in the regional atmosphere over urban areas across the United States. The public health questions associated with ultrafine particles emitted by natural gas combustion have wide-ranging implications. Similar levels of ultrafine particle concentrations will likely occur in other regions across the world that extensively use natural gas as a fuel source, although other sources of ultrafine particles may also make strong contributions depending on the total mix of fuels in each region.

Recent theories suggest that primary particulate matter composed of semi-volatile organic compounds may evaporate after release to the atmosphere, which may reduce ambient ~~PNC~~N_x. Measurements conducted in parallel with the current study confirmed that particles emitted from natural gas combustion in home appliances partially evaporated when diluted by a factor of 25 in clean air, but particles emitted from reciprocating engines ~~industrial sources~~ did not evaporate under the same conditions (Xue et al., 2018a). Future work should verify the accuracy of the size and composition distributions for all natural gas combustion sources given their apparent importance for predicted ~~PNC~~N_x.

Evidence from both toxicology and epidemiology will be required to assess the effect of UFPs on public health. It is essential to identify and quantify UFP sources based on both mass ($PM_{0.1}$) and ~~number PNC~~N_x during this process (Friend et al., 2013). An accurate comparison of both $PM_{0.1}$ and ~~PNC~~ N_x exposure could lay the groundwork for specific assessment of health effects of UFPs and potentially more efficient control strategies for PM emission from major sources (Yue et al., 2008). Ideally, spatial exposure patterns for ~~PNC~~N_x, $PM_{0.1}$, and $PM_{2.5}$ will be sufficiently unique to separate their individual effects in epidemiological studies. Regression statistics for different metrics were calculated by

using all grid cells in the model domain of the current study. The correlations between the various particle metrics were: R^2($PM_{2.5}$ vs. ~~PNC~~N_{10})=0.35, R^2($PM_{2.5}$ vs. $PM_{0.1}$)=0.63, R^2($PM_{0.1}$ vs. ~~PNC~~N_{10})=0.75. It seems likely that future epidemiological studies will be able to differentiate between the effects of $PM_{2.5}$ and ~~PNC~~ N_x based on the low R^2 value. The potential for comparisons between $PM_{2.5}$ and $PM_{0.1}$ is less clear cut, but previous work helps understand what may be possible. Ostro et al. (2015) compared the associations between IHD mortality and $PM_{2.5}$ vs. $PM_{0.1}$ in the California Teachers Study (CTS) cohort. Associations between IHD mortality and the sum of $PM_{2.5}$ mass (p-value=0.001) were stronger than associations between IHD mortality and the sum of $PM_{0.1}$ mass (p-value=0.01) but individual components of mass (EC, OC, Cu, etc) all had stronger associations with IHD mortality in the $PM_{0.1}$ size fraction than the $PM_{2.5}$ size fraction.

The current study focuses on outdoor exposure to UFPs that may be useful in future epidemiological studies. Indoor or in-vehicle exposure to UFPs can also be significant (Wallace and Ott, 2011;Rim et al., 2010;Bhangar et al., 2011;Weichenthal et al., 2015;Fruin et al., 2008) but characterizing these micro-environments is beyond the scope of the current manuscript.

5. Conclusions

The UCD/CIT regional chemical transport model has been updated with a nucleation algorithm and combined with the existing size-resolved source profiles of particlualte matter emissions to predict regional source contributions to airborne particle number concentration (~~PNC~~N_{10}) and airborne particulate ultrafine mass ($PM_{0.1}$). Predicted 24-hour average ~~PNC~~ N_{10} follows the same trend as ~~is in good agreement with~~ measured N_{7}~~-1000~~ at ten sites across California in summer (Aug) and winter (Dec). Predicted diurnal variation of ~~PNC~~ N_{10} follows the same trend as ~~is in reasonable agreement with~~ measured concentrations at the majority of the evaluation sites in August and December, but the results suggest that further refinement is needed for both primary emissions and nucleation algorithms. ~~but uner-predicts early evening peaks in the winter due to the failure of meteorological calculations to capture the suppressed mixing in the atmosphere~~

~~at these times.~~ Predicted $PM_{0.1}$ source contributions follow the same trends as ~~are in good agreement with~~ $PM_{0.1}$ source contributions measured in a molecular marker study at four sites across California in summer (August) and winter (December) months. Natural gas combustion is the largest primary source of regional ~~PNC~~ N_{10} at all locations outside of the immediate vicinity of other major combustion sources. Nucleation contributed strongly to particle number during both the summer and winter months ~~at midday but did not dominate PNC concentrations~~. ~~Likewise, t~~Traffic sources contributed to ~~PNC~~ N_{10} but did not dominate over regions more than 300 m away from freeways. Combustion sources such as wood burning, food cooking, and mobile sources made stronger contributions to $PM_{0.1}$ at heavily urbanized locations. Wood burning for home heating had strong seasonal patterns with peak concentrations in winter while other sources contributed more consistently throughout the seasons. Nucleation made a negligible contribution to $PM_{0.1}$ over the urban areas at the focus of the current study.

The current study identifies natural gas combustion as an important ~~major~~ source of ultrafine particle number and mass concentrations in urban regions throughout California. The health implications of these natural gas combustion particles should be investigated in future epidemiology studies.

Data Availability: All of the $PM_{0.1}$ and ~~PNC~~ N_x outdoor exposure fields produced in the current study are available free of charge at http://faculty.engineering.ucdavis.edu/kleeman/ which provides a link to the most recent version of the dataset (currently http://webwolf.engr.ucdavis.edu/data/soa_v2/monthly_avg2). Model source code and model input files are available to collaborators via direct email to the corresponding author at mjkleeman@ucdavis.edu.

Acknowledgements: This research was supported by the Bay Area Air Quality Management District under project #2013.218, the Coordinating Research Council under project #A-96, and the California Air Resources Board under project #14-314. None of the project sponsors nor any person acting on their behalf: (1) makes any warranty,

Formatted: Not Highlight

Formatted: Not Highlight

Formatted: Not Highlight

express or implied, with respect to the use of any information, apparatus, method, or process disclosed in this report, or (2) assumes any liabilities with respect to use, or damages resulting from the use or inability to use, any information, apparatus, method, or process disclosed in this report.

Reference

Anttila, T., and Kerminen, V. M.: Condensational growth of atmospheric nuclei by organic vapours, Journal of Aerosol Science, 34, 41-61, 10.1016/s0021-8502(02)00155-6, 2003.

Bhangar, S., Mullen, N. A., Hering, S. V., Kreisberg, N. M., and Nazaroff, W. W.: Ultrafine particle concentrations and exposures in seven residences in northern California, Indoor Air, 21, 132-144, 10.1111/j.1600-0668.2010.00689.x, 2011.

Boylan, J. W., and Russell, A. G.: PM and light extinction model performance metrics, goals, and criteria for three-dimensional air quality models, Atmos Environ, 40, 4946-4959, 10.1016/j.atmonsenv.2005.09.087, 2006.

Brunekreef, B., and Forsberg, B.: Epidemiological evidence of effects of coarse airborne particles on health, Eur Respir J, 26, 309-318, 2005.

Chen, J. J., Ying, Q., and Kleeman, M. J.: Source apportionment of wintertime secondary organic aerosol during the California regional PM10/PM2.5 air quality study, Atmos Environ, 44, 1331-1340, 2010.

Cooper, J. A. E. A.: Dinal AppendixV-G,PM10 source composition

library for the South Coast Air Basin, South Coast Air Quality Management District, Diamond Bar, California, 1989.

Dockery, D. W., and Stone, P. H.: Cardiovascular risks from fine particulate air pollution, New Engl J Med, 356, 511-513, 2007.

Elleman, R. A., and Covert, D. S.: Aerosol size distribution modeling with the Community Multiscale Air Quality modeling system in the Pacific Northwest: 2. Parameterizations for ternary nucleation and nucleation mode processes, J Geophys Res-Atmos, 114, 2009a.

Elleman, R. A., and Covert, D. S.: Aerosol size distribution modeling with the Community Multiscale Air Quality modeling system in the Pacific Northwest: 1. Model comparison to observations, J Geophys Res-Atmos, 114, 2009b.

Fann, N., Lamson, A. D., Anenberg, S. C., Wesson, K., Risley, D., and Hubbell, B. J.: Estimating the National Public Health Burden Associated with Exposure to Ambient PM2.5 and Ozone, Risk Anal, 32, 81-95, 2012.

Friend, A. J., Ayoko, G. A., Jager, D., Wust, M., Jayaratne, E. R., Jamriska, M., and Morawska, L.: Sources of ultrafine particles and chemical species along a traffic corridor: comparison of the results from two receptor models, Environ Chem, 10, 54-63, 2013.

Fruin, S., Westerdahl, D., Sax, T., Sioutas, C., and Fine, P. M.: Measurements and predictors of on-road ultrafine particle concentrations and associated pollutants in Los Angeles, Atmos Environ, 42, 207-219, 10.1016/j.atmosenv.2007.09.057, 2008.

Gauderman, W. J., Urman, R., Avol, E., Berhane, K., McConnell, R., Rappaport, E., Chang, R., Lurmann, F., and Gilliland, F.: Association of Improved Air Quality with Lung Development in Children, New Engl J Med, 372, 905-913, 2015.
Gu, J. W., Pitz, M., Schnelle-Kreis, J., Diemer, J., Reller, A., Zimmermann, R., Soentgen, J., Stoelzel, M., Wichmann, H. E., Peters, A., and Cyrys, J.: Source apportionment of ambient particles: Comparison of positive matrix factorization analysis applied to particle size distribution and chemical composition data, Atmos Environ, 45, 1849-1857, 2011.
Harley, R. A., Hannigan, M. P., and Cass, G. R.: Respeciation of Organic Gas Emissions and the Detection of Excess Unburned Gasoline in the Atmosphere, Environmental science & technology, 26, 2395-2408, DOI 10.1021/es00036a010, 1992.
Held, T., Ying, Q., Kaduwela, A., and Kleeman, M.: Modeling particulate matter in the San Joaquin Valley with a source-oriented externally mixed three-dimensional photochemical grid model, Atmos Environ, 38, 3689-3711, 2004.
Held, T., Ying, Q., Kleeman, M. J., Schauer, J. J., and Fraser, M. P.: A comparison of the UCD/CIT air quality model and the CMB source-receptor model for primary airborne particulate matter, Atmos Environ, 39, 2281-2297, 2005.
Hildemann, L. M., Markowski, G. R., and Cass, G. R.: Chemical-Composition of Emissions from Urban Sources of Fine Organic Aerosol, Environmental science & technology, 25, 744-759, DOI 10.1021/es00016a021, 1991a.
Hildemann, L. M., Markowski, G. R., Jones, M. C., and Cass, G. R.: Submicrometer Aerosol Mass Distributions of Emissions from Boilers, Fireplaces, Automobiles, Diesel Trucks, and Meat-Cooking Operations, Aerosol Sci Tech, 14, 138-152, Doi 10.1080/02786829108959478, 1991b.
Hildemann, L. M., G.R. Markowski, and G.R. Cass: Chemical composition of emissions from urban sources of fine organic aerosol, Environmental Science and Technology, 25, 744-759, 1991.
Hixson, M., Mahmud, A., Hu, J. L., Bai, S., Niemeier, D. A., Handy, S. L., Gao, S. Y., Lund, J. R., Sullivan, D. C., and Kleeman, M. J.: Influence of regional development policies and clean technology adoption on future air pollution exposure, Atmos Environ, 44, 552-562, 2010.
Hixson, M., Mahmud, A., Hu, J., and Kleeman, M. J.: Resolving the interactions between population density and air pollution emissions controls in the San Joaquin Valley, USA, Journal of the Air & Waste Management Association, 62, 566-575, 10.1080/10962247.2012.663325, 2012.
Houck, J. E., Chow, J. C., Watson, J. G., Simons, C. A., Prichett,, and L. C., G., J. M., Frazier, C. A.: Determination of particle size distribution and chemical composition of particulate matter from selected sources in California, California Air Resources Board, OMNI Environment Service Incorporate, Desert Research Institute, Beaverton, Oregon, 1989.
Hu, J., Howard, C. J., Mitloehner, F., Green, P. G., and Kleeman, M. J.: Mobile source and livestock feed contributions to regional ozone formation in Central California, Environmental science & technology, 46, 2781-2789, 10.1021/es203369p, 2012.
Hu, J., Zhang, H., Chen, S., Ying, Q., Wiedinmyer, C., Vandenberghe, F., and Kleeman, M. J.: Identifying PM2.5 and PM0.1 sources for epidemiological studies in California, Environmental science & technology, 48, 4980-4990, 10.1021/es404810z, 2014a.
Hu, J., Zhang, H., Chen, S. H., Wiedinmyer, C., Vandenberghe, F., Ying, Q., and Kleeman, M. J.: Predicting primary PM2.5 and PM0.1 trace composition for epidemiological studies in California, Environmental science & technology, 48, 4971-4979, 10.1021/es404809j, 2014b.
Hu, J., Zhang, H., Ying, Q., Chen, S. H., Vandenberghe, F., and Kleeman, M. J.: Long-term particulate matter modeling for health effect studies in California – Part 1: Model performance on temporal and spatial variations, Atmospheric Chemistry and Physics, 15, 3445-3461, 10.5194/acp-15-3445-2015, 2015.

Hu, J. L., Jathar, S., Zhang, H. L., Ying, Q., Chen, S. H., Cappa, C. D., and Kleeman, M. J.: Long-term particulate matter modeling for health effect studies in California - Part 2: Concentrations and sources of ultrafine organic aerosols, Atmospheric Chemistry and Physics, 17, 5379-5391, 2017.
Hudda, N., Gould, T., Hartin, K., Larson, T. V., and Fruin, S. A.: Emissions from an International Airport Increase Particle Number Concentrations 4-fold at 10 km Downwind, Environmental Science & Technology, 48, 6628-6635, 10.1021/es5001566, 2014.
Jung, J. G., Pandis, S. N., and Adams, P. J.: Evaluation of nucleation theories in a sulfur-rich environment, Aerosol Sci Tech, 42, 495-504, 2008.
Jung, J. G., Fountoukis, C., Adams, P. J., and Pandis, S. N.: Simulation of in situ ultrafine particle formation in the eastern United States using PMCAMx-UF, J Geophys Res-Atmos, 115, 2010.
Kasumba, J., Hopke, P. K., Chalupa, D. C., and Utell, M. J.: Comparison of sources of submicron particle number concentrations measured at two sites in Rochester, NY, Sci Total Environ, 407, 5071-5084, 2009.
Kerminen, V. M., and Kulmala, M.: Analytical formulae connecting the "real" and the "apparent" nucleation rate and the nuclei number concentration for atmospheric nucleation events, J Aerosol Sci, 33, 609-622, 2002.
Kleeman, M. J., Cass, G. R., and Eldering, A.: Modeling the airborne particle complex as a source-oriented external mixture, J Geophys Res-Atmos, 102, 21355-21372, 1997.
Kleeman, M. J., and Cass, G. R.: Source contributions to the size and composition distribution of urban particulate air pollution, Atmos Environ, 32, 2803-2816, 1998.
Kleeman, M. J., Schauer, J. J., and Cass, G. R.: Size and composition distribution of fine particulate matter emitted from wood burning, meat charbroiling, and cigarettes, Environmental science & technology, 33, 3516-3523, 10.1021/es981277q, 1999.
Kleeman, M. J., Schauer, J. J., and Cass, G. R.: Size and composition distribution of fine particulate matter emitted from motor vehicles, Environmental science & technology, 34, 1132-1142, 10.1021/es981276y, 2000.
Kleeman, M. J., and Cass, G. R.: A 3D Eulerian source-oriented model for an externally mixed aerosol, Environmental science & technology, 35, 4834-4848, 2001.
Kleeman, M. J., Ying, Q., Lu, J., Mysliwiec, M. J., Griffin, R. J., Chen, J. J., and Clegg, S.: Source apportionment of secondary organic aerosol during a severe photochemical smog episode, Atmos Environ, 41, 576-591, 2007.
Kleeman, M. J., Robert, M. A., Riddle, S. G., Fine, P. M., Hays, M. D., Schauer, J. J., and Hannigan, M. P.: Size distribution of trace organic species emitted from biomass combustion and meat charbroiling (vol 42, pg 3059, 2008), Atmos Environ, 42, 6152-6154, 2008a.
Kleeman, M. J., Robert, M. A., Riddle, S. G., Fine, P. M., Hays, M. D., Schauer, J. J., and Hannigan, M. P.: Size distribution of trace organic species emitted from biomass combustion and meat charbroiling, Atmos Environ, 42, 3059-3075, 10.1016/j.atmosenv.2007.12.044, 2008b.
Kuwayama, T., Collier, S., Forestieri, S., Brady, J. M., Bertram, T. H., Cappa, C. D., Zhang, Q., and Kleeman, M. J.: Volatility of Primary Organic Aerosol Emitted from Light Duty Gasoline Vehicles, Environmental Science & Technology, 49, 1569-1577, 2015.
Laurent, O., Hu, J., Li, L., Kleeman, M. J., Bartell, S. M., Cockburn, M., Escobedo, L., and Wu, J.: A Statewide Nested Case-Control Study of Preterm Birth and Air Pollution by Source and Composition: California, 2001-2008, Environ Health Perspect, 124, 1479-1486, 10.1289/ehp.1510133, 2016.
Li, N., Sioutas, C., Cho, A., Schmitz, D., Misra, C., Sempf, J., Wang, M. Y., Oberley, T., Froines, J., and Nel, A.: Ultrafine particulate pollutants induce oxidative stress and mitochondrial damage, Environ Health Persp, 111, 455-460, 2003.

Li, W., and Hopke, P. K.: Initial Size Distributions and Hygroscopicity of Indoor Combustion Aerosol Particles, Aerosol Sci Tech, 19, 305-316, 10.1080/02786829308959638, 1993.
Lupascu, A., Easter, R., Zaveri, R., Shrivastava, M., Pekour, M., Tomlinson, J., Yang, Q., Matsui, H., Hodzic, A., Zhang, Q., and Fast, J. D.: Modeling particle nucleation and growth over northern California during the 2010 CARES campaign, Atmospheric Chemistry and Physics, 15, 12283-12313, 2015.
Mahmud, A., Hixson, M., Hu, J., Zhao, Z., Chen, S. H., Kleeman, M. J.: Climate impact on airborne particulate matter concentrations in California using seven year analysis periods, Atmospheric Chemistry and Physics, 10, 11097-11114, 10.5194/acp-10-11097-2010, 2010.
May, A. A., Levin, E. J. T., Hennigan, C. J., Riipinen, I., Lee, T., Collett, J. L., Jimenez, J. L., Kreidenweis, S. M., and Robinson, A. L.: Gas-particle partitioning of primary organic aerosol emissions: 3. Biomass burning, J Geophys Res-Atmos, 118, 11327-11338, 2013a.
May, A. A., Presto, A. A., Hennigan, C. J., Nguyen, N. T., Gordon, T. D., and Robinson, A. L.: Gas-particle partitioning of primary organic aerosol emissions: (1) Gasoline vehicle exhaust, Atmospheric Environment, 77, 128-139, 2013b.
Mazaheri, M., Johnson, G. R., and Morawska, L.: Particle and Gaseous Emissions from Commercial Aircraft at Each Stage of the Landing and Takeoff Cycle, Environmental science & technology, 43, 441-446, 10.1021/es8013985, 2009.
Miller, K. A., Siscovick, D. S., Sheppard, L., Shepherd, K., Sullivan, J. H., Anderson, G. L., and Kaufman, J. D.: Long-term exposure to air pollution and incidence of cardiovascular events in women, New Engl J Med, 356, 447-458, 2007.
Montagne, D. R., Hoek, G., Klompmaker, J. O., Wang, M., Meliefste, K., and Brunekreef, B.: Land Use Regression Models for Ultrafine Particles and Black Carbon Based on Short-Term Monitoring Predict Past Spatial Variation, Environmental science & technology, 49, 8712-8720, 2015.
Morawska, L., Ristovski, Z., Jayaratne, E. R., Keogh, D. U., and Ling, X.: Ambient nano and ultrafine particles from motor vehicle emissions: Characteristics, ambient processing and implications on human exposure, Atmos Environ, 42, 8113-8138, 2008.
Mysliwiec, M. J., and Kleeman, M. J.: Source apportionment of secondary airborne particulate matter in a polluted atmospbere, Environmental science & technology, 36, 5376-5384, 2002.
Napari, I., Noppel, M., Vehkamaki, H., and Kulmala, M.: Parametrization of ternary nucleation rates for H(2)SO(4)-NH(3)-H(2)O vapors, J Geophys Res-Atmos, 107, 2002.
Nel, A., Xia, T., Madler, L., and Li, N.: Toxic potential of materials at the nanolevel, Science, 311, 622-627, 2006.
Oberdorster, G., Sharp, Z., Atudorei, V., Elder, A., Gelein, R., Lunts, A., Kreyling, W., and Cox, C.: Extrapulmonary translocation of ultrafine carbon particles following whole-body inhalation exposure of rats, J Toxicol Env Heal A, 65, 1531-1543, 2002.
Ogulei, D., Hopke, P. K., Chalupa, D. C., and Utell, M. J.: Modeling source contributions to submicron particle number concentrations measured in Rochester, New York, Aerosol Sci Tech, 41, 179-201, 2007.
Ostro, B., Broadwin, R., Green, S., Feng, W. Y., and Lipsett, M.: Fine particulate air pollution and mortality in nine California counties: Results from CALFINE, Environ Health Persp, 114, 29-33, 2006.
Ostro, B., Lipsett, M., Reynolds, P., Goldberg, D., Hertz, A., Garcia, C., Henderson, K. D., and Bernstein, L.: Long-Term Exposure to Constituents of Fine Particulate Air Pollution and Mortality: Results from the California Teachers Study, Environ Health Persp, 118, 363-369, 2010.
Ostro, B., Hu, J., Goldberg, D., Reynolds, P., Hertz, A., Bernstein, L., and Kleeman, M. J.: Associations of mortality with long-term exposures to fine and ultrafine particles, species and

sources: results from the California Teachers Study Cohort, Environ Health Perspect, 123, 549-556, 10.1289/ehp.1408565, 2015.
Otte, T. L.: The impact of nudging in the meteorological model for retrospective air quality simulations. Part II: Evaluating collocated meteorological and air quality observations, J Appl Meteorol Clim, 47, 1868-1887, 10.1175/2007jamc1791.1, 2008a.
Otte, T. L.: The impact of nudging in the meteorological model for retrospective air quality simulations. Part I: Evaluation against national observation networks, J Appl Meteorol Clim, 47, 1853-1867, 10.1175/2007jamc1790.1, 2008b.
Pope, C. A., Burnett, R. T., Thun, M. J., Calle, E. E., Krewski, D., Ito, K., and Thurston, G. D.: Lung cancer, cardiopulmonary mortality, and long-term exposure to fine particulate air pollution, Jama-J Am Med Assoc, 287, 1132-1141, 2002.
Pope, C. A., Burnett, R. T., Thurston, G. D., Thun, M. J., Calle, E. E., Krewski, D., and Godleski, J. J.: Cardiovascular mortality and long-term exposure to particulate air pollution - Epidemiological evidence of general pathophysiological pathways of disease, Circulation, 109, 71-77, 2004.
Pope, C. A., Ezzati, M., and Dockery, D. W.: Fine-Particulate Air Pollution and Life Expectancy in the United States., New Engl J Med, 360, 376-386, 2009.
Rasmussen, D. J., Hu, J. L., Mahmud, A., and Kleeman, M. J.: The Ozone-Climate Penalty: Past, Present, and Future, Environmental science & technology, 47, 14258-14266, 2013.
Rim, D. H., Wallace, L., and Persily, A.: Infiltration of Outdoor Ultrafine Panicles into a Test House, Environmental science & technology, 44, 5908-5913, 2010.
Robert, M. A., Kleeman, M. J., and Jakober, C. A.: Size and composition distributions of particulate matter emissions: Part 2- Heavy-duty diesel vehicles, Journal of the Air & Waste Management Association, 57, 1429-1438, 2007a.
Robert, M. A., VanBergen, S., Kleeman, M. J., and Jakober, C. A.: Size and composition distributions of particulate matter emissions: Part 1 - Light-duty gasoline vehicles, Journal of the Air & Waste Management Association, 57, 1414-1428, 2007b.
Schauer, J. J., Kleeman, M. J., Cass, G. R., and Simoneit, B. R. T.: Measurement of emissions from air pollution sources. 2. C-1 through C-30 organic compounds from medium duty diesel trucks, Environmental science & technology, 33, 1578-1587, DOI 10.1021/es980081n, 1999a.
Schauer, J. J., Kleeman, M. J., Cass, G. R., and Simoneit, B. R. T.: Measurement of emissions from air pollution sources. 1. C-1 through C-29 organic compounds from meat charbroiling, Environmental science & technology, 33, 1566-1577, DOI 10.1021/es980076j, 1999b.
Schauer, J. J., Kleeman, M. J., Cass, G. R., and Simoneit, B. R. T.: Measurement of emissions from air pollution sources. 3. C-1-C-29 organic compounds from fireplace combustion of wood, Environmental science & technology, 35, 1716-1728, DOI 10.1021/es001331e, 2001.
Schauer, J. J., Kleeman, M. J., Cass, G. R., and Simoneit, B. R. T.: Measurement of emissions from air pollution sources. 5. C-1-C-32 organic compounds from gasoline-powered motor vehicles, Environmental science & technology, 36, 1169-1180, 10.1021/es0108077, 2002a.
Schauer, J. J., Kleeman, M. J., Cass, G. R., and Simoneit, B. R. T.: Measurement of emissions from air pollution sources. 4. C-1-C-27 organic compounds from cooking with seed oils, Environmental science & technology, 36, 567-575, 10.1021/es002053m, 2002b.
Shet, C. S., Cholemari, M. R., and Veeravalli, S. V.: Eulerian spatial and temporal autocorrelations: assessment of Taylor's hypothesis and a model, Journal of Turbulence, 1-15, 10.1080/14685248.2017.1357823, 2017.
Sioutas, C., Delfino, R. J., and Singh, M.: Exposure assessment for atmospheric ultrafine particles (UFPs) and implications in epidemiologic research, Environ Health Persp, 113, 947-955, 2005.

Sowlat, M. H., Hasheminassab, S., and Sioutas, C.: Source apportionment of ambient particle number concentrations in central Los Angeles using positive matrix factorization (PMF), Atmospheric Chemistry and Physics, 16, 4849-4866, 10.5194/acp-16-4849-2016, 2016.
Taback, H. J., Brienza, A. R., Macko, J., and Brunetz, N.: Fine particle emissions from stationary and miscellaneous sources in the South Coast Air Basin. KVB Report 5806-783., KVB Incorporated, Tustin, California, 1979.
Trostl, J., Chuang, W. K., Gordon, H., Heinritzi, M., Yan, C., Molteni, U., Ahlm, L., Frege, C., Bianchi, F., Wagner, R., Simon, M., Lehtipalo, K., Williamson, C., Craven, J. S., Duplissy, J., Adamov, A., Almeida, J., Bernhammer, A. K., Breitenlechner, M., Brilke, S., Dias, A., Ehrhart, S., Flagan, R. C., Franchin, A., Fuchs, C., Guida, R., Gysel, M., Hansel, A., Hoyle, C. R., Jokinen, T., Junninen, H., Kangasluoma, J., Keskinen, H., Kim, J., Krapf, M., Kurten, A., Laaksonen, A., Lawler, M., Leiminger, M., Mathot, S., Mohler, O., Nieminen, T., Onnela, A., Petaja, T., Piel, F. M., Miettinen, P., Rissanen, M. P., Rondo, L., Sarnela, N., Schobesberger, S., Sengupta, K., Sipila, M., Smith, J. N., Steiner, G., Tome, A., Virtanen, A., Wagner, A. C., Weingartner, E., Wimmer, D., Winkler, P. M., Ye, P. L., Carslaw, K. S., Curtius, J., Dommen, J., Kirkby, J., Kulmala, M., Riipinen, I., Worsnop, D. R., Donahue, N. M., and Baltensperger, U.: The role of low-volatility organic compounds in initial particle growth in the atmosphere, Nature, 533, 527-+, 10.1038/nature18271, 2016.
Venecek, M., Yu, X., and Kleeman, M.: Ultrafine Particulate Matter Source Contributions across the Continental United States, Atmospheric Chemistry and Physics, submitted for review, 2018.
Wallace, L., and Ott, W.: Personal exposure to ultrafine particles, J Expo Sci Environ Epidemiol, 21, 20-30, 10.1038/jes.2009.59, 2011.
Wang, Z. B., Hu, M., Wu, Z. J., Yue, D. L., He, L. Y., Huang, X. F., Liu, X. G., and Wiedensohler, A.: Long-term measurements of particle number size distributions and the relationships with air mass history and source apportionment in the summer of Beijing, Atmospheric Chemistry and Physics, 13, 10159-10170, 2013.
Watson, J. G., Chow, J. C., Sodeman, D. A., Lowenthal, D. H., Chang, M. C. O., Park, K., and Wang, X.: Comparison of four scanning mobility particle sizers at the Fresno Supersite, Particuology, 9, 204-209, 10.1016/j.partic.2011.03.002, 2011.
Weichenthal, S., Van Ryswyk, K., Kulka, R., Sun, L., Wallace, L., and Joseph, L.: In-vehicle exposures to particulate air pollution in Canadian metropolitan areas: the urban transportation exposure study, Environmental science & technology, 49, 597-605, 10.1021/es504043a, 2015.
Westervelt, D. M., Pierce, J. R., Riipinen, I., Trivitayanurak, W., Hamed, A., Kulmala, M., Laaksonen, A., Decesari, S., and Adams, P. J.: Formation and growth of nucleated particles into cloud condensation nuclei: model-measurement comparison, Atmospheric Chemistry and Physics, 13, 7645-7663, 2013.
Xue, J., Li, Y., Peppers, J., Wan, C., Kado, N., Green, P. G., Young, T., and Kleeman, M.: Ultrafine particle emissions from natural gas, biogas and biomethane combustion, Environmental Science and Technology, in review, 2018a.
Xue, J., Xue, W., Sowlat, M., Sioutas, C., Lilinco, A., Hasson, A., and Kleeman, M.: Annual trends in ultrafine particulate matter (PM0.1) source contributions in polluted California cities, Environmental Science and Technology, in preparation, 2018b.
Ying, Q., and Kleeman, M. J.: Source contributions to the regional distribution of secondary particulate matter in California, Atmos Environ, 40, 736-752, 2006.
Ying, Q., Lu, J., Allen, P., Livingstone, P., Kaduwela, A., and Kleeman, M.: Modeling air quality during the California Regional PM10/PM2.5 Air Quality Study (CRPAQS) using the UCD/CIT source-oriented air quality model - Part I. Base case model results, Atmos Environ, 42, 8954-8966, 2008a.

Ying, Q., Lu, J., Kaduwela, A., and Kleeman, M.: Modeling air quality during the California Regional PM10/PM2.5 Air Quality Study (CPRAQS) using the UCD/CIT Source Oriented Air Quality Model - Part II. Regional source apportionment of primary airborne particulate matter, Atmos Environ, 42, 8967-8978, 2008b.

Yue, W., Stolzel, M., Cyrys, J., Pitz, M., Heinrich, J., Kreyling, W. G., Wichmann, H. E., Peters, A., Wang, S., and Hopke, P. K.: Source apportionment of ambient fine particle size distribution using positive matrix factorization in Erfurt, Germany, Sci Total Environ, 398, 133-144, 2008.

Zhang, H. L., and Ying, Q.: Source apportionment of airborne particulate matter in Southeast Texas using a source-oriented 3D air quality model, Atmos Environ, 44, 3547-3557, 2010.

Zhang, K. M., Wexler, A. S., Zhu, Y. F., Hinds, W. C., and Sioutas, C.: Evolution of particle number distribution near roadways. Part II: the 'road-to-ambient' process, Atmospheric Environment, 38, 6655-6665, 10.1016/j.atmosenv.2004.06.044, 2004.

Zhang, K. M., Wexler, A. S., Niemeier, D. A., Zhu, Y. F., Hinds, W. C., and Sioutas, C.: Evolution of particle number distribution near roadways. Part III: Traffic analysis and on-road size resolved particulate emission factors, Atmospheric Environment, 39, 4155-4166, 10.1016/j.atmosenv.2005.04.003, 2005.

Zhang, Y., Liu, P., Liu, X. H., Jacobson, M. Z., McMurry, P. H., Yu, F. Q., Yu, S. C., and Schere, K. L.: A comparative study of nucleation parameterizations: 2. Three-dimensional model application and evaluation, J Geophys Res-Atmos, 115, 10.1029/2010jd014151, 2010.

Zhao, Z., Chen, S. H., Kleeman, M. J., Tyree, M., and Cayan, D.: The Impact of Climate Change on Air Quality-Related Meteorological Conditions in California. Part I: Present Time Simulation Analysis, J Climate, 24, 3344-3361, 2011.

Zhu, Y. F., Hinds, W. C., Kim, S., Shen, S., and Sioutas, C.: Study of ultrafine particles near a major highway with heavy-duty diesel traffic, Atmospheric Environment, 36, 4323-4335, 10.1016/s1352-2310(02)00354-0, 2002a.

Zhu, Y. F., Hinds, W. C., Kim, S., and Sioutas, C.: Concentration and size distribution of ultrafine particles near a major highway, Journal of the Air & Waste Management Association, 52, 1032-1042, 10.1080/10473289.2002.10470842, 2002b.